93-10-18

IEA Industrial Electrical Engineering and Automation
Lund Institute of Technology

# Oscillations in Inverter Fed Induction Motor Drives

Bo Peterson

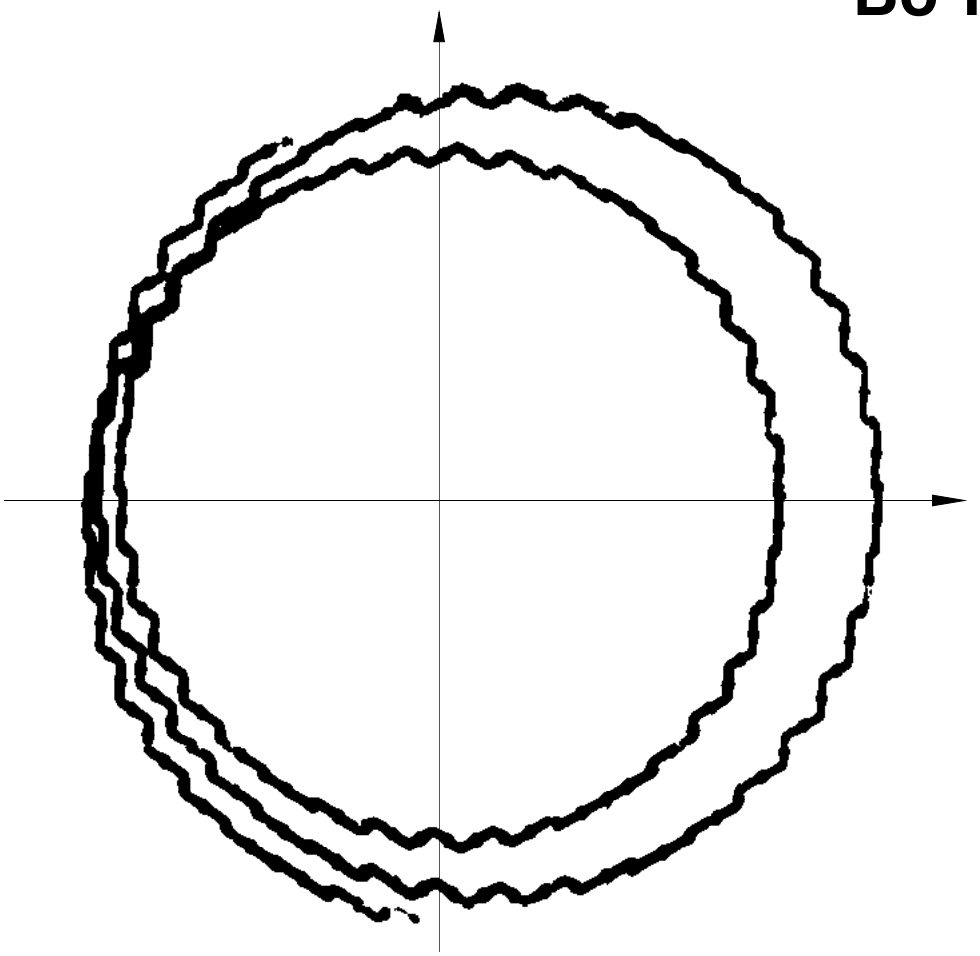

September 1991

# Oscillations in Inverter Fed Induction Motor Drives

Bo Peterson

Lund 1991

Department of
Industrial Electrical Engineering and
Automation (IEA)
Lund Institute of Technology
Box 118
S-221 00 LUND
Sweden

*Issuing organization*
Department of Industrial Electrical Engineering and Automation (IEA),
Lund Institute of Technology

*Document name*
Tekn. Lic. Dissertation

*Date of issue*
Sep 1991

*Document number*
CODEN: LUTEDX/(TEIE-1001)/1-67/(1991)

*Author(s)*
Bo Peterson

*Supervisor*
Gustaf Olsson, Jaroslav Valis

*Sponsoring organization*

*Title and subtitle*
Oscillations in Inverter Fed Induction Motor Drives

*Abstract*

Severe oscillations in the range of 1 to 100 Hz have been encountered in inverter fed induction motor drive systems, especially where there are no external damping loads, such as fan drives. These oscillations may damage the drive system or generate noise. It is found that the induction machine has two resonance frequencies. The damping of the first resonance is decreased with increased stator resistance, while the damping of the second resonance is increased with increased stator resistance. Simple mechanical models are presented which give physical insight into the reason for the oscillations, as well as suggestions of how to suppress them.

*Key words*
Instability, Resonance, Induction machine, Inverter, Mechanical model

*Classification system or index terms*

*Supplementary bibliographical information*

*ISSN and key title*

*ISBN*

*Language*
English

*Number of pages*
67

*Recipient's notes*

*Security classification*

The document may be ordered from: IEA, Box 118, S-221 00 LUND, Sweden

# Abstract

Severe oscillations in the range of 1 to 100 Hz have been encountered in inverter fed induction motor drive systems, especially where there are no external damping loads, such as fan drives. These oscillations may damage the drive system or generate noise. It is found that the induction machine has two resonance frequencies. The damping of the first resonance is decreased with increased stator resistance, while the damping of the second resonance is increased with increased stator resistance. Simple mechanical models are presented which give physical insight into the reason for the oscillations, as well as suggestions of how to suppress them.

# Contents

# Acknowledgements

I was introduced to the problem of oscillating induction machines in 1990 by Professor Jaroslav Valis and Tommy Magnusson, both at the Department of Industrial Electrical Engineering and Automation, together with Claus Holm Hansen, at that time working for Speed Control A/S, Denmark. I am very thankful for their support during my work and I also thank Professor František Bernát at the Czechoslovak Academy of Sciences for supplying me with background material. Last but not least I thank my supervisor Professor Gustaf Olsson who has helped and encouraged me through my work.

# 1 Introduction

Oscillatory behaviour of electrical machines in certain applications - also known as instability or hunting - is a well-known topic. The conditions under which a DC motor exhibits an oscillatory response to a sudden change of its supply voltage or load is a common issue in any textbook on electrical machines (Fitzgerald et al 1985). The oscillatory behaviour of synchronous machines is also well known and understood (Wagner 1930). Stepper motors are ill-famed for their poorly damped oscillating response.

## Oscillations in Induction Machines

The oscillatory behaviour of line-fed induction motors in constant speed applications has also been noticed long time ago, however less well understood. The reason is probably that the induction motor is an intricate electro-magnetic-mechanical system, difficult to analyze and describe in purely electrical terms. The classical T-shaped per-phase equivalent diagram describes the induction motor at steady state, giving no hint on the dynamic behaviour.

Only recently, using the space vector method, a profound analysis of the oscillations is found (Kovács 1984). Kovács has analyzed overshoot after acceleration, response to a sudden load change, forced oscillations excited by load fluctuations, and has derived expressions for the natural frequency and damping of oscillations. His expressions are not valid at all times however, due to some limiting assumptions, for example that the stator resistance is equal to zero.

Kovács' formulas exposed the fact that the typical resonance frequencies were in the range of 1 to 100 Hz, i.e. within the usual range of motor speeds in inverter-fed variable speed drives. This is the reason why problems caused by instability has become more accentuated in variable speed drives.

## Observations of Oscillations

Excessive oscillations at certain motor speeds are actually encountered in many applications, especially when the load itself can not provide sufficient mechanical damping, as fan blowers, or when the load torque contains a periodic component, as a

piston compressor, which can excite the oscillations. The oscillations may also be excited by fluctuations of the air gap torque due to imperfections in the motor, as eccentricity and slotting.

### Induction Machines Connected to Inverters

It has been observed that large motors (> 10 kW) oscillate more than small ones (< 2 kW), motors with low inertia more than motors with a large-inertia load. The motor inductances have an influence on the resonance frequency. The influence of winding resistances on damping is puzzling; some engineers have observed that the damping increased with a higher stator resistance, others have found the contrary. In motors connected to inverters, the DC link capacitor influences both the damping and the resonance frequencies.

When testing different brands of motors and inverters in a particular application it has been noticed that some inverter-motor combinations are more prone to oscillations than others.

Most inverters with simple PWM open loop control have a tendency to generate a torque fluctuation with a frequency six times of that of the motor frequency, exciting oscillations.

Imperfections in the power stage such as differences between individual switches, switching times and dead times will cause torque fluctuations that can excite oscillations. This is accentuated when high switching frequency is used.

### Analysis of the Oscillations

Various attempts have been made to analyze and explain the causes of these oscillations. A straightforward solution would seem to be to describe the whole drive system consisting of the inverter, the motor and the load by a set of ordinary differential equations, to find the eigenvalues and to identify the modes of oscillations, natural frequencies and damping. However, the motor is a multivariable non-linear continuous system, and the load itself may be a complex mechanical system. All this makes a straightforward analysis and its interpretation difficult.

To make the system more transparent it has to be simplified. A standard way is to linearize the system for a certain operating point - a certain slip for example - to be able to apply the theory of linear systems for its analysis. This method was attempted by many researchers (Palit 1978; Alexandrovitz 1987).

Unfortunately, it is an almost hopeless task to derive algebraic expressions for the eigenvalues of a matrix of this size. A numerical solution does not give any physical insight into the oscillatory behaviour.

Another way to simplify the problem is to use an electro-mechanical analogy to describe the induction machine. Interpreting the mathematical model of the induction motor as an equivalent mechanical system reveals that an induction itself is a poorly damped oscillating system, whose two resonance frequencies depend on the motor flux, the leakage and the magnetizing inductance and rotor moment of inertia. The damping is only due to the winding resistances.

When the motor is fed from an inverter the DC link capacitor becomes part of the oscillating system and can also be included in the mechanical model.

### Damping of the Oscillations

Methods for suppressing the oscillations using electronics have been presented (Mutoh et al 1990) but they are often more complicated than necessary. However, with a good understanding of the physical reasons for the resonance, and some additional feedback, the resonance problems can be solved in a better way.

This thesis suggests an efficient yet simple way of damping torque oscillations disrupting the function of induction motors that are fed and controlled by inverters.

The new idea is to introduce an electronic damping by a fast acting control of the angular frequency of the stator flux vector. A control law based on feedback of the current in the DC link is derived and its properties are verified by simulations.

### Outline of the Thesis

In section 2 the fundamental dynamic equations of the induction machine are described. Section 3 presents a mechanical analogy to the dynamic equations. Sections 4 and 5 describe how to determine the resonance frequencies experimentally. Section 6 and 7 examine the physical reasons for the oscillations. In section 8 the resonance is discussed in terms of eigenvalues of a linearized system. Finally it is shown how feedback can damp the oscillations.

# 2 Dynamic Behaviour

The dynamic behaviour of an induction machine can be described by three vector differential equations in a reference frame attached to the stator (Kovács 1984):

$$\frac{d\bar{\Psi}_s}{dt} = \bar{u}_s - \bar{i}_s R_s \tag{2.1}$$

$$\frac{d\bar{\Psi}_r}{dt} = j\omega\bar{\Psi}_r - \bar{i}_r R_r \tag{2.2}$$

$$J\ \frac{d\omega}{dt} = Im(\bar{\Psi}_s^* \bar{i}_s) - T_m \tag{2.3}$$

with the two algebraic conditions

$$\bar{\Psi}_s = \bar{i}_s(L_{sl} + L_m) + \bar{i}_r L_m = \bar{i}_s L_s + \bar{i}_r L_m \tag{2.4}$$

$$\bar{\Psi}_r = \bar{i}_s L_m + \bar{i}_r(L_{rl} + L_m) = \bar{i}_s L_m + \bar{i}_r L_r \tag{2.5}$$

The equations are in *per unit* (p.u.) notation. (The terminology and the derivation of the p.u.-values are found in App. A). The stator current vector and stator voltage vector are

$$\bar{i}_s = \frac{2}{3}(i_a + \bar{a} i_b + \bar{a}^2 i_c) \tag{2.6}$$

$$\bar{u}_s = \frac{2}{3}(u_a + \bar{a} u_b + \bar{a}^2 u_c) \tag{2.7}$$

where

$$\bar{a} = \mathrm{e}^{j\,2\pi/3} \tag{2.8}$$

$u_a$, $u_b$ and $u_c$ are instantaneous values of phase-to-neutral voltages, $i_a$, $i_b$ and $i_c$ are instantaneous values of line currents.

The system of equations is non-linear and it is difficult to see the reasons for the oscillations in the equations. If the equations were linear, the eigenvalues could be calculated, but they wouldn't give any clue to why the oscillations occur.

As was mentioned before, attempts have been made to gain understanding of the oscillations by manipulating the vector equations, but as the system of equations is a non-linear system of the fifth order, this method has many disadvantages.

However, a mechanical equivalent of the mathematical model can be used to gain a better intuitive understanding of the induction machine. The approach in this thesis is to derive apparent mechanical equivalent model representations that give physical explanations for the oscillations, as well as ways of computing numerical values of resonance frequencies and damping.

# 3 Mechanical Model

A mechanical model of equations (2.4-2.5) is shown in Fig. 3.1, where inductances have become springs and currents are forces pulling the springs (Török et al 1985). The inductance is the inverse of the stiffness of the spring. (App. E gives a complete description of corresponding parameters in the electrical and mechanical models.)

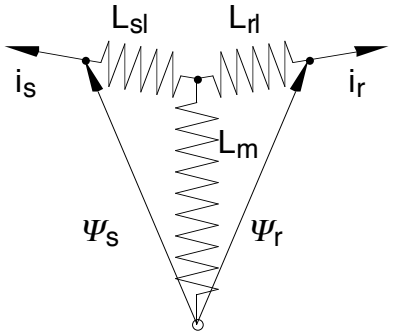


Figure 3.1 Mechanical model of equations (2.4-2.5)

The linked fluxes are vectors with a length and a direction corresponding to the original fluxes. It is seen that the torque on the springs developed by the current $\bar{i}_s$ is

$$Im\ (\bar{\Psi}_s^* \bar{i}_s) = T \tag{3.1}$$

which is the driving torque in equation (2.3). The point in Fig. 3.1 where the force $\bar{i}_r$ is attached to the spring $L_{rl}$ follows the restrictions of equation (2.2). The resistance $R_r$ is represented as a viscous damper which can be a drag-pad on an oily surface. The velocity difference between the drag-pad and the surface is proportional to the force applied to the drag-pad, and the velocity and the force have the same direction. The time derivative of the flux in the mechanical model is the velocity of the tip of the flux vector.

If the oily surface is a rotating disc with the angular speed $\omega$ (Fig. 3.2) then the relative velocity difference between the drag-pad and the disc is

$$\bar{v}_{diff} = \frac{d\bar{\Psi}_r}{dt} - j\omega\bar{\Psi}_r \tag{3.2}$$

The force on the drag-pad is $-\bar{i}_r$ and then the velocity difference between the disc and the drag-pad can be expressed as

$$\bar{v}_{diff} = -\bar{i}_r R_r \tag{3.3}$$

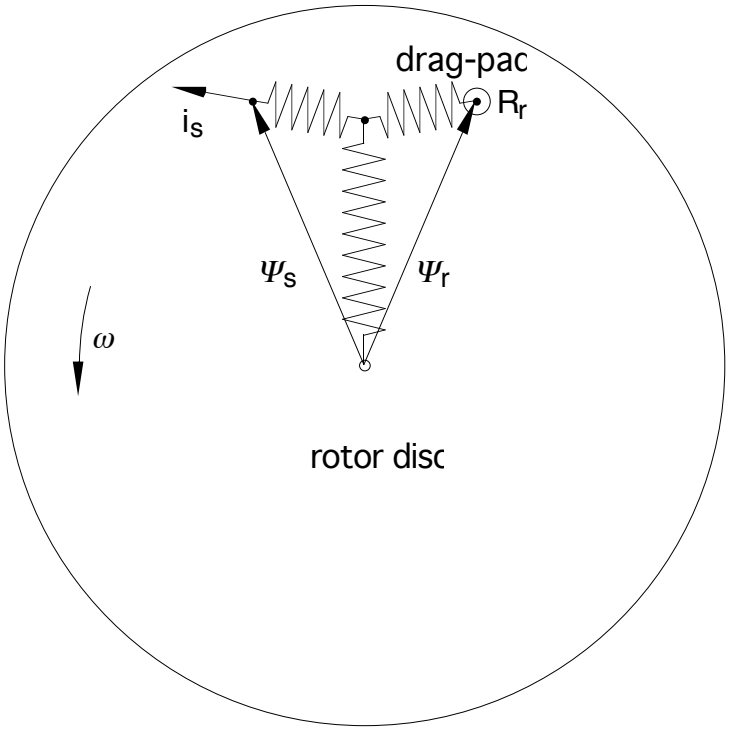


Figure 3.2 Mechanical model of equations (2.2-2.5)

Combining equations (3.2) and (3.3) gives equation (3.4),

$$\frac{d\bar{\Psi}_r}{dt} = j\omega\bar{\Psi}_r - \bar{i}_r R_r \tag{3.4}$$

The torque transferred from the drag-pad to the disc is given by equation (3.1),

$$Im\,(\bar{\Psi}_s^* \bar{i}_s) = T. \tag{3.5}$$

If the rotating disc represents the rotor and has the actual rotor moment of inertia, we have an *exact* mechanical analogy of equations (2.2-2.5). To get a complete analogy of equations (2.1-2.5), the stator resistance must be modelled.

## Mechanical Model of the Stator Resistance

Equation (2.1) can also be represented by a mechanical equivalent. The term $\bar{i}_s \square R_s$ is represented as a drag-pad on a viscous surface. The drag-pad is transferring the force $\bar{i}_s$ to the springs. The viscous surface is moving with the velocity $\bar{u}_s$ independently of the stator flux. All points of this surface are moving in the same direction at the same speed. Contrary to the rotor disc, this surface can not rotate. The velocity of the tip of the stator flux will be the difference between the stator voltage and the resistive voltage-drop in the stator. Figure 3.3 shows the mechanical model with the stator resistance included.

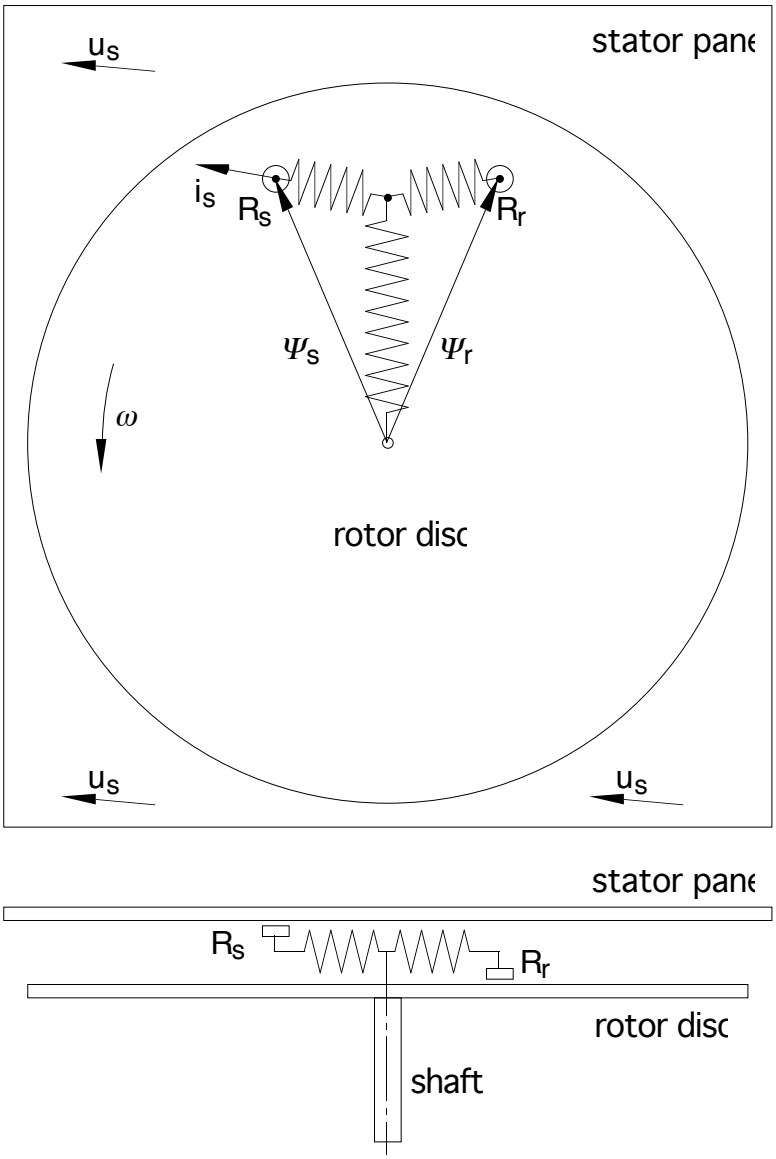


Figure 3.3 Mechanical model with the stator resistance included

## Mechanical Model with Fewer Parameters

It is possible to get an equivalent mechanical model of Fig. 3.2, with fewer parameters than the original one. A few simple transformations have to be done. The same transformations can be done to the traditional T-shaped per-phase equivalent circuit of the stationary motor, to get a model with fewer parameters (Slemon et al 1980).

In a squirrel-cage induction motor it is impossible to separate the stator leakage inductance from the rotor leakage inductance. One of the parameters is redundant and models with one total leakage inductance instead of two separate ones can be obtained. Various models can be derived. In the model described below, the values of the inductances correspond to the values that are obtained from no-load and locked-rotor tests.

The original model is shown in Fig. 3.4 (a), with the stator and rotor omitted. The two springs $L_{sl}$ and $L_m$ in Fig. 3.4 (b) can be replaced by one spring, $L_T$, and the flux $\Psi_s$ is transformed into $\Psi_T$. This is shown in Fig. 3.4 (c) where

$$\Psi_T = \frac{L_m}{L_m + L_{sl}} \Psi_s \tag{3.6}$$

$$L_T = \frac{L_m}{L_m + L_{sl}} L_{sl} \tag{3.7}$$

Now let

$$\frac{L_m}{L_m + L_{sl}} = k \tag{3.8}$$

This transformation is analogous to using Thévenin's theorem in the electrical circuit of Fig. 3.4 (f). The resistors $R_1$ and $R_2$ can be replaced by $R_T$ if the voltage $U$ is replaced by $U_T$, where

$$R_T = \frac{R_2}{R_1 + R_2} R_1 \text{ and } U_T = \frac{R_2}{R_1 + R_2} U$$

From Fig. 3.4 (d) it is seen that the rotor current vector is

$$\bar{i}_r = \frac{-\bar{\Psi}_T + \bar{\Psi}_r}{L_T + L_{rl}} = \frac{-k\bar{\Psi}_s}{k L_{sl} + L_{rl}} + \frac{\bar{\Psi}_r}{k L_{sl} + L_{rl}} \tag{3.9}$$

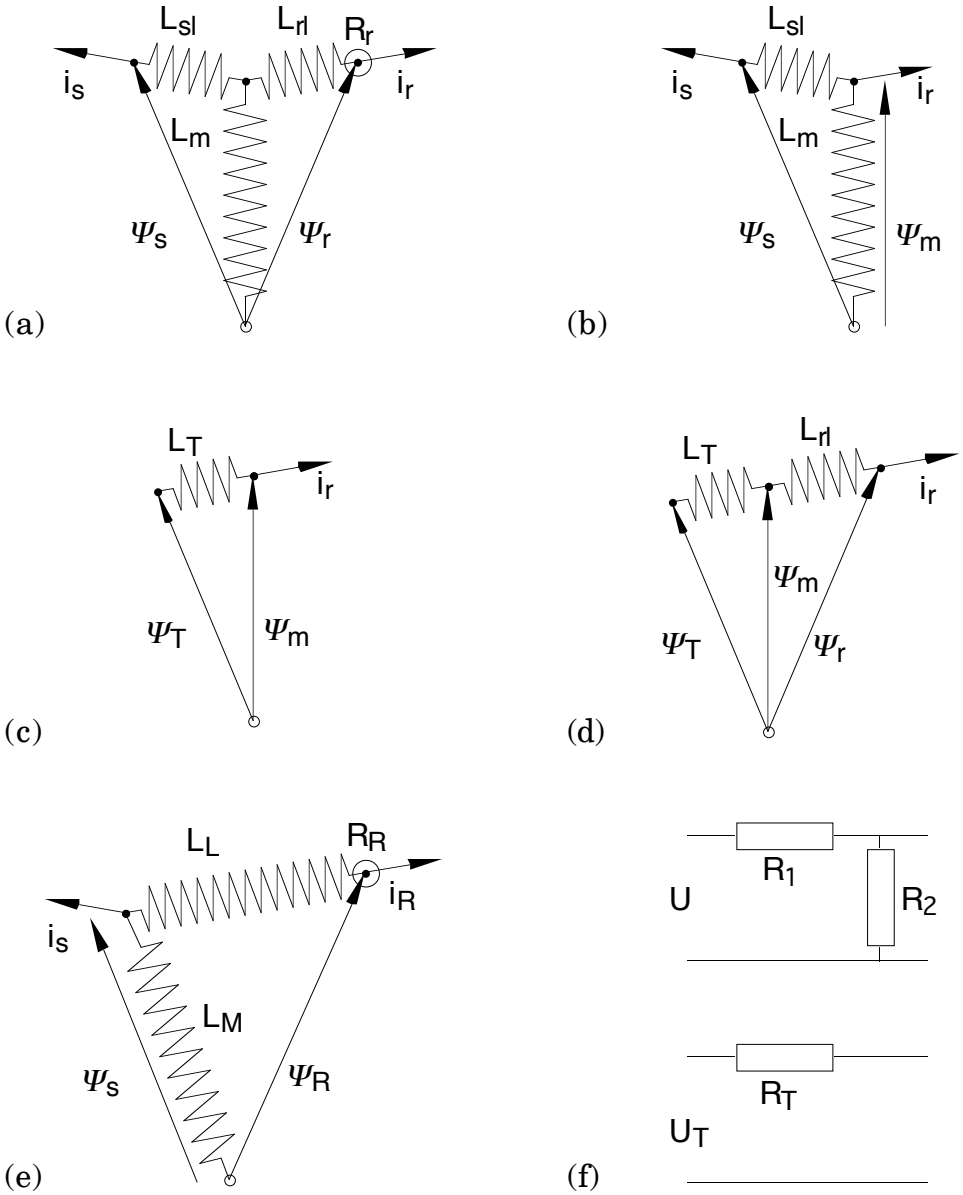


Figure 3.4 Transformations of the mechanical model.

The stator current $\bar{i}_s$ in Fig. 3.4 (b) may be expressed as the sum of two components, one due to the stator flux $\bar{\Psi}_s$, the other due to the rotor current $\bar{i}_r$. If the current $\bar{i}_r$ is set to zero, the first component is

$$\bar{i}_{s1} = \frac{\bar{\Psi}_s}{L_m + L_{sl}} = \frac{k\bar{\Psi}_s}{L_m} \tag{3.10}$$

When the stator flux is set to zero, the second component is

$$\bar{i}_{s2} = -\frac{L_m}{L_m + L_{sl}}\bar{i}_r = -k\,\bar{i}_r \tag{3.11}$$

Thus by superposition,

$$\bar{i}_s = \bar{i}_{s1} + \bar{i}_{s2} = \frac{k\bar{\Psi}_s}{L_{sl}} - k\,\bar{i}_r \tag{3.12}$$

By substitution from equation (3.9),

$$\bar{i}_s = \frac{\bar{\Psi}_s}{L_m/k} + \frac{\bar{\Psi}_s}{L_{sl}/k + L_{rl}/k^2}\frac{\bar{\Psi}_r/k}{L_{sl}/k + L_{rl}/k^2}$$

$$= \frac{\bar{\Psi}_s}{L_M} + \frac{\bar{\Psi}_s}{L_L} - \frac{\bar{\Psi}_R}{L_L} \tag{3.13}$$

where

$$L_M = \frac{L_m}{k} \tag{3.14}$$

$$L_L = \frac{L_{sl}}{k} + \frac{L_{rl}}{k^2} \tag{3.15}$$

$$\bar{\Psi}_R = \frac{\bar{\Psi}_r}{k} \tag{3.16}$$

Equation (3.13) describes the model in Fig. 3.4 (e). The rotor resistance must also be transformed. Equation (2.2),

$$\frac{d\bar{\Psi}_r}{dt} = j\omega\bar{\Psi}_r - \bar{i}_r R_r$$

must be replaced by

$$\frac{d\bar{\Psi}_R}{dt} = j\omega\bar{\Psi}_R - \bar{i}_R R_R \tag{3.17}$$

where

$$\bar{i}_R = -\bar{i}_{s2} = k\,\bar{i}_r \tag{3.18}$$

Equation (3.16) implies that

$$\frac{d\bar{\Psi}_R}{dt} = \frac{1}{k}\frac{d\bar{\Psi}_r}{dt} = \frac{1}{k}j\omega\bar{\Psi}_r - \frac{1}{k}\bar{i}_r R_r = j\omega\bar{\Psi}_R - \frac{1}{k^2}\bar{i}_R R_r \quad (3.19)$$

Now the last parameter is found to be

$$R_R = \frac{R_r}{k^2} \quad (3.20)$$

and the model in Fig. 3.4 (e) is an exact equivalent of the model in Fig. 3.4 (a). The complete improved model with the rotor disc included is shown in Fig. 3.5. Due to the resemblance to the Greek letter Γ, this model is sometimes referred to as the Γ-model.

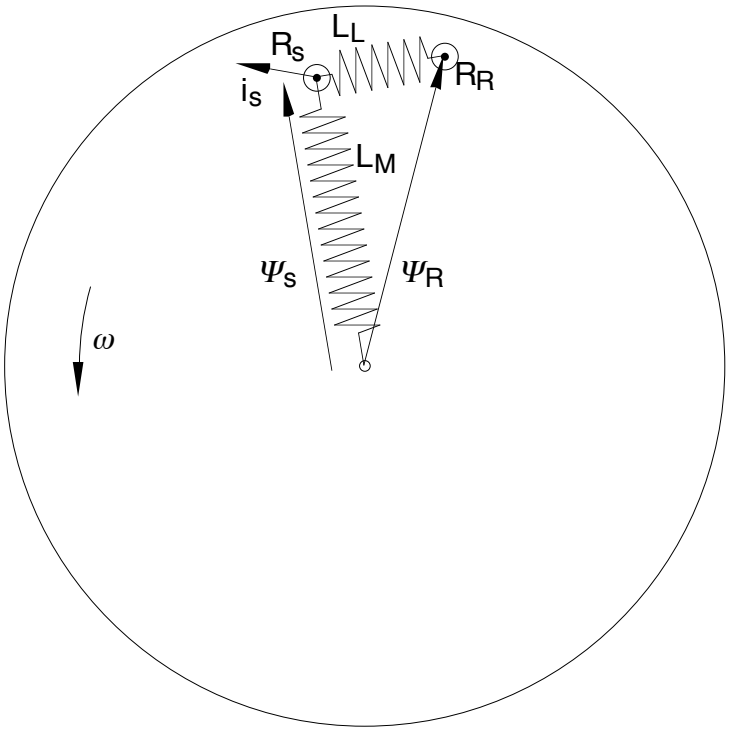


Figure 3.5. Mechanical Γ-model

The stator equation is equal to the that of the original model, which leads to the final set of equations (compare equations (2.1-2.5)):

$$\frac{d\bar{\Psi}_s}{dt} = \bar{u}_s - \bar{i}_s R_s \tag{3.21}$$

$$\frac{d\bar{\Psi}_R}{dt} = j\omega\bar{\Psi}_R - \bar{i}_R R_R \tag{3.22}$$

$$J \frac{d\omega}{dt} = Im(\bar{\Psi}_s^* \bar{i}_s) - T_m \tag{3.23}$$

$$\bar{\Psi}_s = (\bar{i}_s + \bar{i}_R) L_M \tag{3.24}$$

$$\bar{\Psi}_R = \bar{\Psi}_s + \bar{i}_R L_L \tag{3.25}$$

The relations between the models are:

| Γ-model | | original model | |
|---|---|---|---|
| $L_M$ | = | $\frac{L_m}{k}$ | (3.26) |
| $L_L$ | = | $\frac{L_{sl}}{k} + \frac{L_{rl}}{k^2}$ | (3.27) |
| $R_s$ | = | $R_s$ | (3.28) |
| $R_R$ | = | $\frac{R_r}{k^2}$ | (3.29) |
| $\bar{\Psi}_s$ | = | $\bar{\Psi}_s$ | (3.30) |
| $\bar{\Psi}_R$ | = | $\frac{\bar{\Psi}_r}{k}$ | (3.31) |
| $\bar{i}_s$ | = | $\bar{i}_s$ | (3.32) |
| $\bar{i}_R$ | = | $k\,\bar{i}_r$ | (3.33) |

$$k = \frac{L_m}{L_m + L_{sl}} \tag{3.34}$$

Note that the vectors $\bar{\Psi}_r$ and $\bar{\Psi}_R$ have the same arguments, only the magnitudes are different. This is also true for $\bar{i}_r$ and $\bar{i}_R$.

# 4 Experimental Set-up

With a simple experimental set-up, the oscillatory behaviour of the induction machine can be investigated. With this test, two resonance frequencies can be distinguished. The test is performed with a non-rotating rotor. However, the rotor is not locked, but free to oscillate.

The machine is magnetized in one direction to rated flux by a DC-current, flowing through two of the phases of the stator winding. A voltage source with variable frequency is applied to the third phase, exciting the machine in a direction perpendicular to the DC-flux (Fig. 4.1). The voltage source may be a function generator connected to an audio power amplifier.

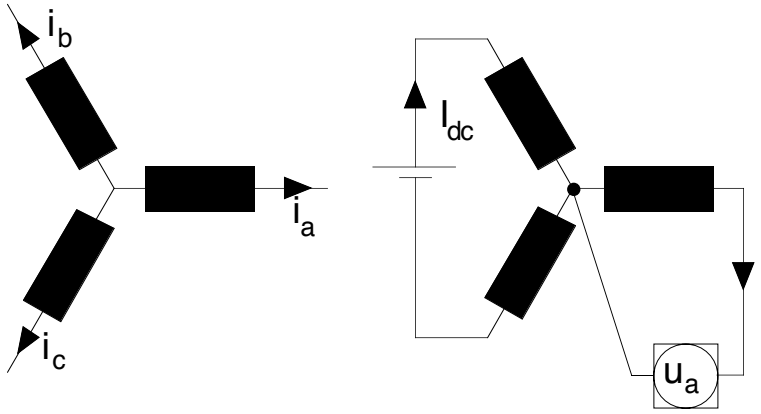


Figure 4.1 DC-excited induction machine

With vector representation of the induction machine, the DC-current and voltage become the components of the stator current and voltage in the imaginary axis direction. The stator current vector and stator voltage vector are

$$\bar{i}_s = \frac{2}{3}(i_a + \bar{a} i_b + \bar{a}^2 i_c) \tag{4.1}$$

$$\bar{u}_s = \frac{2}{3}(u_a + \bar{a} u_b + \bar{a}^2 u_c) \tag{4.2}$$

where

$$\bar{a} = e^{j\,2\pi/3} \tag{4.3}$$

$u_a$, $u_b$ and $u_c$ are instantaneous values of phase-to-neutral voltages, $i_a$, $i_b$ and $i_c$ are instantaneous values of line currents, all in p.u.-notation.

If the line currents are $i_b = -I_{dc}$ and $i_c = I_{dc}$ then the imaginary parts of the stator current and voltage vectors are

$$i_{sy} = -\frac{2}{\sqrt{3}} I_{dc} \tag{4.4}$$

$$u_{sy} = R_s\, i_{sy} \tag{4.5}$$

The current needed for rated flux $\Psi = 1$ p.u. is

$$|\, i_{sy}\,| = \frac{\Psi}{L_M} \tag{4.6}$$

The frequency of the voltage $u_a$ is varied and the the current $i_a$ is measured. The rotor is free to move and will oscillate with the same frequency as the voltage.

The voltage $u_a$ in vector representation becomes the voltage in the real axis direction

$$u_{sx} = \frac{2}{3} u_a \tag{4.7}$$

The current $I_{dc}$ needed for rated flux can be calculated in two ways, either by combining equations (4.4) and (4.6) which gives

$$I_{dc} = \frac{\sqrt{3}}{2} \frac{\Psi}{L_M} \tag{4.8}$$

or by using information on the rating plate of the machine. The rated current consists of two parts, one magnetizing current and one torque generating current. The torque generating current is equal to the rated current multiplied by rated $\cos\varphi$ and the magnetizing current is the rated current multiplied by rated $\sin\varphi$,

$$i_{magn} = I_n \sin\varphi = |\, i_{sy}\,| \tag{4.9}$$

where $I_n$ is the *peak-value* of the rated current. Equation (4.4) and (4.9) together with $I_{n,rms} = I_n/\sqrt{2}$ give

$$I_{dc} = \sqrt{\frac{3}{2}}\; I_{n,rms} \sin\varphi \tag{4.10}$$

At low frequencies, the induction machine will behave as an inductive load i.e. the current $i_a$ lags the voltage $u_a$. As the frequency is increased, the phase angle is reduced, and the machine will behave as a capacitive load i.e. the current leads the voltage. This is due to the moment of inertia of the rotor, acting as a capacitance. When the frequency is further increased, the motor will behave as an inductive load again.

The frequencies where the current changes from lagging to leading, and from leading to lagging are the two resonance frequencies. The current is low at the first frequency, as in the case of parallel resonance. The current is high at the second frequency as in series resonance.

In the following sections the two kinds of resonance will be referred to as *parallel* resonance and *series* resonance.

# 5 Measurements

The measurements described in section 4 have been performed on a Y-connected 1.1 kW two-pole motor from Grundfos. The data of the motor are found in App. B.

Table 5.1 shows the measured data, where $f$ is the frequency of the feeding voltage $u_a$ and the line current $i_a$ shown in Fig. 4.1. The values of $u_a$ and $i_a$ are peak values in natural units. According to equation (4.7), $u_{sx} = 2/3\ u_a$, and the p.u.-value is obtained if this is divided by the nominal voltage $U_n$. Thus,

$$u_{sx} = \frac{2}{3}\frac{u_a}{U_n} \tag{5.1}$$

Similarly, $i_{sx}$ can be calculated,

$$i_{sx} = \frac{2}{3}\frac{i_a}{I_n} \tag{5.2}$$

The nominal values are $U_n$ = 310 V and $I_n$ = 3.82 A. $\theta$ is the phase angle between $u_a$ and $i_a$ ($\theta > 0$ if $i_a$ leads $u_a$). The last column shows the gain from $u_{sx}$ to $i_{sx}$.

The value of the magnetizing current was (equation (4.10))

$$I_{dc} = \sqrt{\frac{3}{2}}\, I_{n,rms} \sin\varphi = \sqrt{\frac{3}{2}} \cdot 2.7 \cdot \sqrt{1 - \cos^2\varphi} = 1.8 \text{ A}$$

Plots of the gain, $20 \cdot \log(i_{sx}/u_{sx})$, versus the frequency $f$ in p.u., and the phase angle $\theta$ versus the frequency are found in Fig. 5.1. The two resonance frequencies can be clearly distinguished where the phase curve crosses the zero line, the first at about $f$ = 0.2 p.u. (10 Hz) and the second at $f$ = 0.7 p.u. (35 Hz). It is also seen that the gain curve has a minimum at the parallel resonance frequency, and a maximum at the series resonance frequency.

In the following sections, models for the two kinds of resonance will be developed, as well as expressions for calculation of the resonance frequencies.

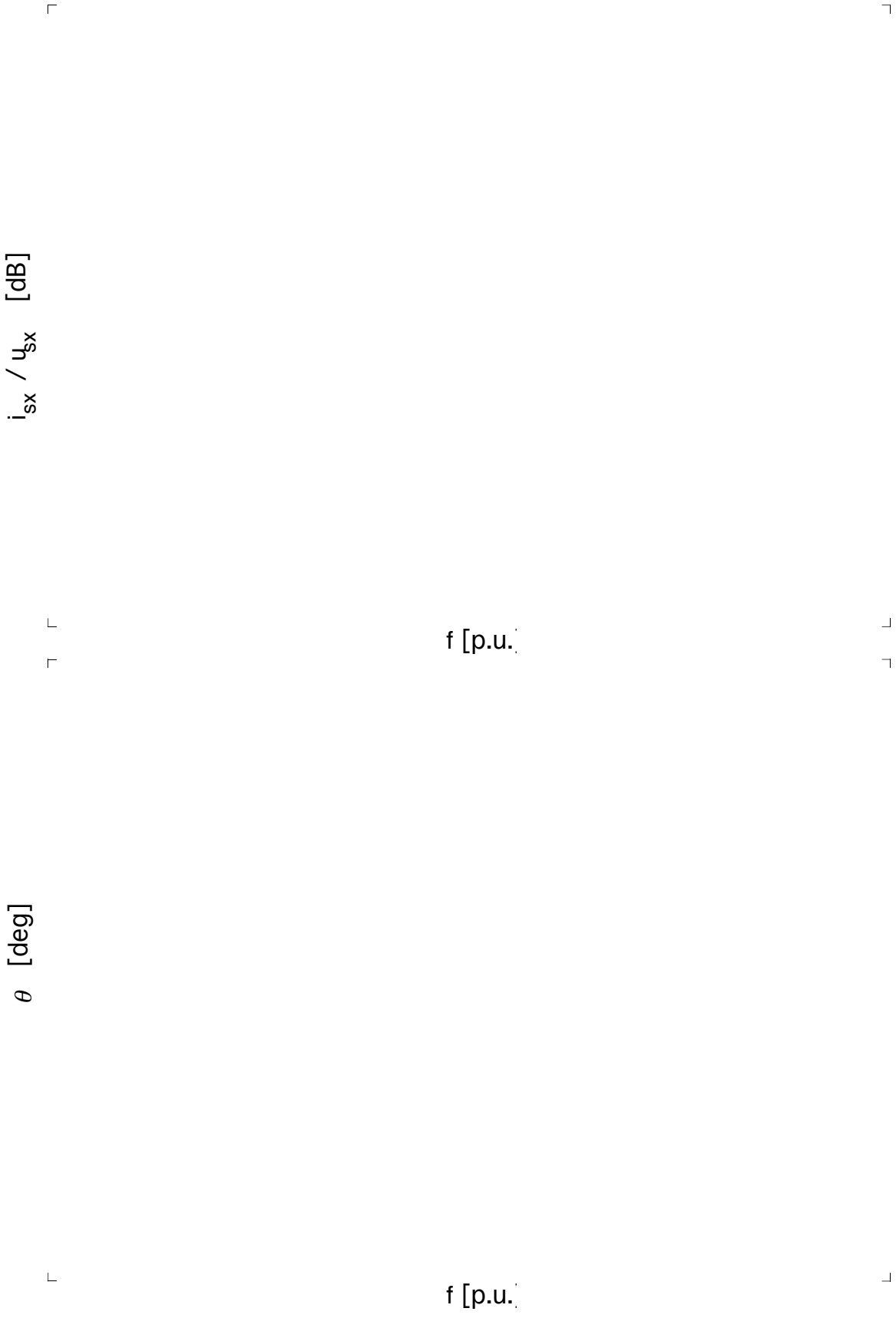


Figure 5.1 Measured gain and phase angle between voltage and current

| $f$ [Hz] | $f$ [p.u.] | $u_a$ [V] | $u_{sx}$ [p.u.] | $i_a$ [A] | $i_{sx}$ [p.u.] | $\theta$ [deg] | $i_{sx}/u_{sx}$ |
|---|---|---|---|---|---|---|---|
| 5 | 0.10 | 7.0 | 0.015 | 0.378 | 0.0660 | –69 | 4.40 |
| 6 | 0.12 | 7.0 | 0.015 | 0.281 | 0.0490 | –71 | 3.27 |
| 7 | 0.14 | 7.0 | 0.015 | 0.201 | 0.0350 | –72 | 2.33 |
| 8 | 0.16 | 7.0 | 0.015 | 0.126 | 0.0220 | –72 | 1.47 |
| 9 | 0.18 | 7.0 | 0.015 | 0.083 | 0.0145 | –55 | 0.97 |
| 10 | 0.20 | 7.0 | 0.015 | 0.055 | 0.0096 | –20 | 0.64 |
| 11 | 0.22 | 7.0 | 0.015 | 0.070 | 0.0122 | 24 | 0.81 |
| 12 | 0.24 | 7.0 | 0.015 | 0.105 | 0.0184 | 41 | 1.23 |
| 15 | 0.30 | 7.0 | 0.015 | 0.218 | 0.0380 | 48 | 2.53 |
| 20 | 0.40 | 7.0 | 0.015 | 0.372 | 0.0650 | 38 | 4.33 |
| 25 | 0.50 | 7.0 | 0.015 | 0.487 | 0.0850 | 28 | 5.67 |
| 30 | 0.60 | 7.0 | 0.015 | 0.562 | 0.0980 | 16 | 6.53 |
| 35 | 0.70 | 7.0 | 0.015 | 0.596 | 0.1040 | 3 | 6.93 |
| 40 | 0.80 | 7.0 | 0.015 | 0.596 | 0.1040 | –8 | 6.93 |
| 45 | 0.90 | 7.0 | 0.015 | 0.590 | 0.1030 | –15 | 6.87 |
| 50 | 1.00 | 7.0 | 0.015 | 0.567 | 0.0990 | –20 | 6.60 |

Table 5.1 Measured data from the Grundfos motor.

# 6 Series Resonance

A clear mechanical model can be obtained for the series resonance. The leakage inductance of the machine plays an essential role in this oscillation. The magnetizing inductance $L_M$ does not effect this oscillation and can be considered infinite.

At the nominal flux the mechanical model is examined in the tangential direction, and the stator voltage vector is assumed to be perpendicular to the flux. This leads to a model with a series connection between a spring, a mass, and two viscous dampers, as in Fig. 6.1 (a).


(a) (b)

Figure 6.1 Mechanical representation of the series resonance

The spring represents the total leakage inductance $L_L$, the mass represents the rotor moment of inertia, and the dampers the stator and rotor resistances. The two dampers can be replaced by a single damper $R_s + R_R = R$ as in Fig. 6.1 (b). If the flux differs from the nominal flux, the mass $J$ can be replaced by a hoist drum with variable radius $\Psi$ and moment of inertia $J$ (Fig. 6.2 (a)), or by a lever with the mass $J$ attached to its end (Fig. 6.2 (b)).

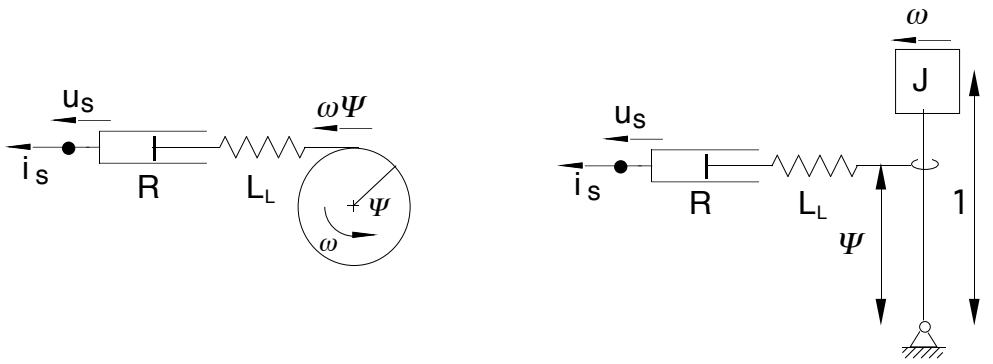


(a) (b)

Figure 6.2 Alternative representations of the series resonance allowing varying flux

The dynamic equations for the system in Fig. 6.2 can be derived either directly from the mechanical system or from the vector equations. The force acting on the mechanical system is represented by the stator current $i_s$. It is seen that

$$\frac{di_s}{dt} = \frac{u_s - Ri_s - \omega\Psi}{L_L} \tag{6.1}$$

$$\frac{d\omega}{dt} = \frac{\Psi_R i_s}{J} \tag{6.2}$$

Another way of deriving these relations is to start with the vector equations in a coordinate system rotating with the angular velocity $\omega_k = 1$. The differential equations (3.21-3.25) have to be changed according to App. D. The real and imaginary parts of the equations become

$$\frac{d\Psi_{sx}}{dt} = u_{sx} - i_{sx} R_s + \Psi_{sy} \tag{6.3}$$

$$\frac{d\Psi_{sy}}{dt} = u_{sy} - i_{sy} R_s - \Psi_{sx} \tag{6.4}$$

$$\frac{d\Psi_{Rx}}{dt} = -\omega\ \Psi_{Ry} - i_{Rx} R_R + \Psi_{Ry} \tag{6.5}$$

$$\frac{d\Psi_{Ry}}{dt} = \omega\ \Psi_{Rx} - i_{Ry} R_R - \Psi_{Rx} \tag{6.6}$$

$$\frac{d\omega}{dt} = \frac{\Psi_{sx} i_{sy} - \Psi_{sy} i_{sx}}{J} \tag{6.7}$$

If $L_M \to \infty$ then $i_s = -i_R$ according to (3.24). At steady state, the flux, voltage and current vectors might appear as in Fig. 6.3.

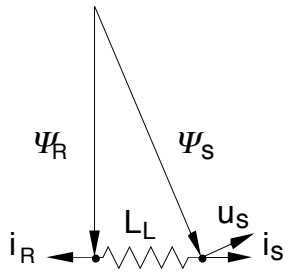


Figure 6.3 Flux, current and voltage vectors at steady state

It is seen in the figure that

$$i_{sy} = i_{Ry} = 0 \tag{6.8}$$

$$i_{Rx} = -\, i_{sx} \tag{6.9}$$

$$\Psi_{Rx} = 0 \tag{6.10}$$

$$\Psi_{sy} = \Psi_{Ry} \tag{6.11}$$

$$i_{sx} = (\Psi_{sx} - \Psi_{Rx})/L_L \tag{6.12}$$

If (6.5) is subtracted from (6.3) and relations (6.8-6.12) are inserted, (6.13) is obtained,

$$L_L \frac{di_{sx}}{dt} = u_{sx} - i_{sx}\,(R_s + R_R) + \omega\Psi_{sy} \tag{6.13}$$

With the following denotation, equation (6.13) is identical to equation (6.1),

$$i_s = i_{sx} \tag{6.14}$$

$$R = R_s + R_R \tag{6.15}$$

$$\Psi = -\,\Psi_{sy} \tag{6.16}$$

$$u_s = u_{sx} \tag{6.17}$$

Equation (6.7) becomes identical to (6.2) with $i_{sy} = 0$,

$$\frac{d\omega}{dt} = \frac{\Psi i_s}{J} \tag{6.18}$$

The system described by (6.1-6.2) can also be described by an equation of the second order,

$$\ddot{\omega} + \frac{R}{L_L}\,\dot{\omega} + \frac{\Psi^2}{JL_L}\,\omega = \frac{u_s \Psi}{JL_L} \tag{6.19}$$

If the characteristic equation

$$s^2 + \frac{R}{L_L}\,s + \frac{\Psi^2}{JL_L} = 0 \tag{6.20}$$

is compared to a standard oscillatory characteristic equation (App. F),

$$s^2 + 2\Omega\zeta\, s + \Omega^2 = 0 \tag{6.21}$$

the natural frequency $\Omega$ of (6.19) is found to be

$$\Omega = \frac{\Psi}{\sqrt{J \cdot L_L}} \tag{6.22}$$

and the relative damping $\zeta$

$$\zeta = \frac{R}{2\Psi}\sqrt{\frac{J}{L_L}} \tag{6.23}$$

It is seen that the damping is decreased with decreasing stator resistance. This is typically a problem for large motors with small relative stator and rotor resistances. In large motors, there is more space for the windings, resulting in a larger copper area, reducing the resistances.

If the parameters of the Grundfos motor described in App. B are inserted into equation (6.22), the natural frequency is

$$\Omega = \frac{\Psi}{\sqrt{J \cdot L_L}} = \frac{1}{\sqrt{13.5 \cdot 0.138}} = 0.733 \text{ p.u.}$$

and the damping is from (6.23)

$$\zeta = \frac{R}{2\Psi}\sqrt{\frac{J}{L_L}} = \frac{0.146}{2}\sqrt{\frac{13.5}{0.138}} = 0.72$$

The frequency in Hz is equal to the frequency in p.u. multiplied by 50 (rated electrical frequency) which gives $f = 37$ Hz, very close to the measured value of 35 Hz in the previous section.

To compare the system described by equation (6.19) with the measured data for other frequencies than the resonance frequency, a Bode plot can be used. As the measured variables are $i_a$ and $u_a$, a transfer function from voltage to current is suitable for comparison. The Laplace transforms of equations (6.18) and (6.19) are

$$s\,W = \frac{\Psi \cdot I_s}{J} \tag{6.24}$$

$$s^2 W + s\frac{R}{L_L}W + \frac{\Psi \cdot \Psi^2}{J \cdot L_L}W = \frac{U_s \cdot \Psi}{J \cdot L_L} \tag{6.25}$$

where $W$ is the Laplace transform of $\omega$.

Combining these equations give the transfer function $H_s$ from $U_s$ to $I_s$, for the series resonance model:

$$I_s = H_s(s)\, U_s = \frac{s/L_L}{s^2 + \frac{R}{L_L}s + \frac{\Psi^2}{JL_L}} U_s \tag{6.26}$$

Amplitude and argument of $H_s(j\omega)$ together with the measured data is found in Fig. 6.4. It is seen that the measured curves (dashed) lie close to the curves of the transfer function $H_s$ (solid) for frequencies greater than 0.4 p.u. (20 Hz).

## Comparison to Earlier Expressions

Oscillations are also discussed in (Kovács 1984). The following characteristic equation is presented:

$$s^2 + s_p\, s + \frac{2T_p}{h} = 0 \tag{6.27}$$

where $s_p$ denotes the pull-out slip, $T_p$ the pull-out torque and $h$ is the moment of inertia in p.u. Note the following differences in the notation used by Kovács and in this thesis:

| | Kovács | Here |
|---|---|---|
| p.u. moment of inertia | $h$ | $J$ |
| p.u. inductance | $X$ | $L$ |

The pull-out torque is defined as

$$T_p = \frac{u_s^2 k^2}{2X_r'} \tag{6.28}$$

and the pull-out slip

$$s_p = \frac{R_r}{X_r'} \tag{6.29}$$

where

$$X_r' = X_{rl} + \frac{X_m X_{sl}}{X_m + X_{sl}} = X_{rl} + k\, X_{sl} \tag{6.30}$$

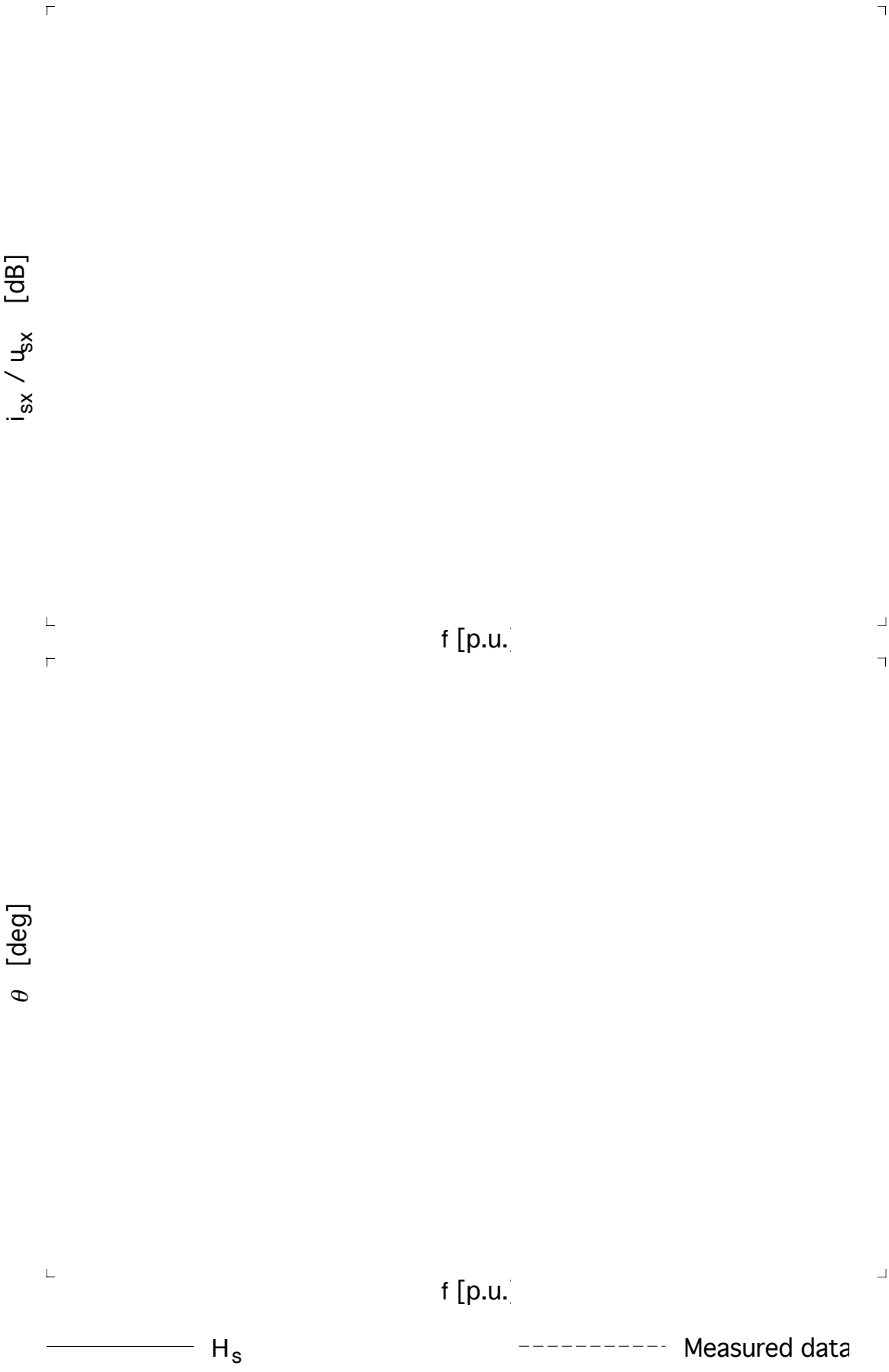


Figure 6.4 Amplitude and argument of transfer function $H_s$

Substituting $h$ by $J$ and $X$ by $L$ and using equations (3.25), (6.28) and (6.30), the term $2T_p/h$ can be written

$$\frac{2T_p}{J} = \frac{2u_s^2 \cdot k^2}{J(2 \cdot \bar{X}_r} \frac{u_s^2}{J} \frac{k^2}{L_{rl}(1 \cdot k) \cdot \bar{L}_s} \frac{u_s^2}{J \cdot L} \tag{6.31}$$

Using (3.29), the term $s_p$ can be written

$$\frac{R_r}{X_r'} = \frac{R_r(1 \cdot}{X_r'(1 \cdot} \frac{k^2 R_R}{\bar{k}^2 L_L} \tag{6.32}$$

Inserting (6.31) and (6.32), the characteristic equation becomes

$$s^2 + \frac{R_R}{L_L} s + \frac{u_s^2}{J \cdot L} = 0 \tag{6.33}$$

which only shows two differences to the characteristic equation (6.20).

In (6.33) the stator voltage $u_s$ is found instead of the flux $\Psi$. This is of no practical importance as the flux is proportional to the stator voltage. Thus, at nominal voltage ($u_s$ = 1), the flux also attains its nominal value ($\Psi$ = 1), and if the voltage is increased or decreased, the magnitude of the flux will follow that of the voltage. Therefore, either the flux or the voltage can be used with exactly the same result.

The other difference is of greatest importance. The sum of stator and rotor resistance in found in (6.20) while only the rotor resistance is found in (6.33). In (Kovács 1984) it is assumed that the stator resistance is zero, and then (6.20) and (6.33) are identical. However, as will be seen later, the influence of the stator resistance can not be neglected. A large stator resistance will reduce the damping of other resonance phenomena.

## Series Resonance with DC Link Capacitor

If the induction motor is connected to an inverter the DC link capacitor becomes part of the oscillating system. The inverter can, as well as the induction machine, be represented by a mechanical model.

The inverter can produce voltage vectors in six directions, and the zero voltage vector, according to Fig. 6.5. The length of the vectors are

$$|u| = \frac{2}{3} U_d \tag{6.34}$$

If the switching frequency is high enough, a voltage vector in any direction can be generated by taking a time average of vectors in two directions and the zero voltage vector.

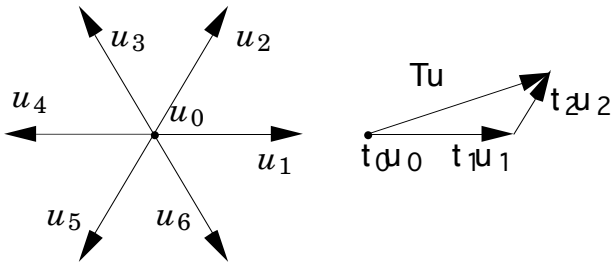


Figure 6.5 Output voltage vectors of an inverter

The zero voltage vector is used during time $t_0$, then $u_1$ is used during $t_1$ and finally $u_2$ during time $t_2$. If $t_0 + t_1 + t_2 = T$ then the average amplitude of the voltage vector during time T is

$$|u| = \frac{\sqrt{(t_1 + 0.5\,t_2)^2 + 0.75\,t_2^2}}{T} \frac{2}{3} U_d \tag{6.35}$$

and the average argument is

$$\alpha = \arccos \frac{t_1 + 0.5\,t_2}{\sqrt{(t_1 + 0.5\,t_2)^2 + 0.75\,t_2^2}}; \; 0 \le \alpha \le 60° \tag{6.36}$$

By choosing another pair of voltage vectors, an arbitrary argument, and an arbitrary amplitude

$$|u| = K\,U_d \le \frac{\sqrt{3}}{2} \frac{2}{3} U_d = \frac{U_d}{\sqrt{3}} \tag{6.37}$$

can be obtained, where $K$ is the amplitude factor (almost the same as duty cycle),

$$K = \frac{\sqrt{(t_1 + 0.5\,t_2)^2 + 0.75\,t_2^2}}{T} \frac{2}{3} \le \frac{t_1 + t_2}{\sqrt{3}} \tag{6.38}$$

Let the average current from the inverter be denoted by $I_d$. The average power from the inverter during time $T$ is

$$P_{inverter} = U_d\,I_d \tag{6.39}$$

and the power to the motor is

$$P_{motor} = \frac{3}{2}(u_{sx}\, i_{sx} + u_{sy}\, i_{sy}) \tag{6.40}$$

The power to the motor must equal the power from the inverter, and it is assumed that $u_{sx} = u_s = KU_d$, $i_{sx} = i_s$ and $i_{sy} = 0$. This leads to

$$I_d = \frac{3}{2} K\, i_s \tag{6.41}$$

A mechanical model can now be obtained for the inverter and its DC link capacitor. The capacitor is modelled by a mass, $m$ = 2C/3. This mass is attached to a lever as in Fig. 6.6 (a).

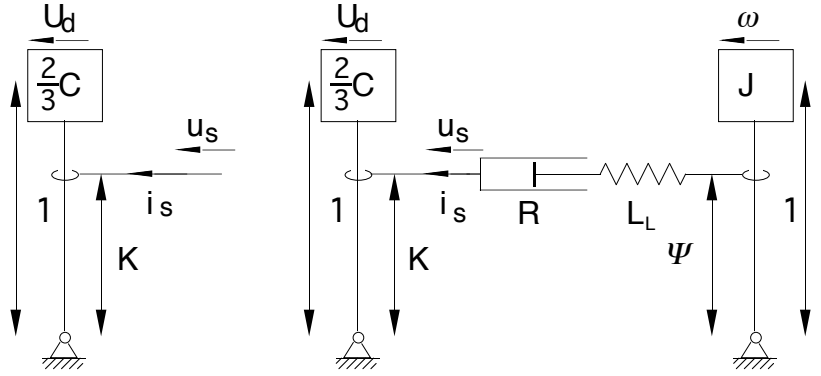


Figure 6.6 (a) Mechanical model of DC link capacitor (b) DC link capacitor connected to induction machine

A model of the inverter connected to the motor model of Fig. 6.2 (b) is seen in Fig. 6.6 (b). The flux is proportional to the the stator voltage $u_s$ and the inverse of the stator frequency $\omega_s$,

$$\Psi = \frac{u_s}{\omega_s} = K\frac{U_d}{\omega_s} \tag{6.42}$$

If the flux is supposed to be constant, $\Psi_o$, the dynamic equations of the system become

$$\frac{di_s}{dt} = \frac{u_s - R \cdot i_s - \omega\Psi_o}{L_L} = \frac{K\sqrt{3}U_d - R \cdot i_s - \omega\Psi_o}{L_L} \tag{6.43}$$

$$\frac{d\omega}{dt} = \frac{i_s \cdot \Psi_o}{J} \tag{6.44}$$

$$\frac{dU_d}{dt} = -\frac{K \cdot i_s}{\frac{2}{\sqrt{3}} \cdot C} \tag{6.45}$$

The equations for this system are non-linear, but can be linearized around an operating point ($i_{so}$, $\omega_o$, $U_{do}$), which results in a system with the state variables

$$x_1 = \delta i_s = i_s - i_{so} \tag{6.46}$$

$$x_2 = \delta\omega = \omega - \omega_o \tag{6.47}$$

$$x_3 = \delta U_d = U_d - U_{do} \tag{6.48}$$

and the input signal

$$u = \delta K = K - K_o \tag{6.49}$$

At steady state the state, we have the following relations for the stator current, angular velocity and flux,

$$i_{so} = 0 \tag{6.50}$$

$$\omega_o = \omega_s \tag{6.51}$$

$$\Psi_o = \frac{K_o U_{do}}{\omega_s} = \frac{K_o U_{do}}{\omega_o} \tag{6.52}$$

The system can now be described by

$$\dot{x} = Ax + Bu \tag{6.53}$$

where

$$A = \begin{bmatrix} -\frac{R}{L_L} & -\frac{\Psi_o}{L_L} & \frac{K_o}{L_L} \\ \frac{\Psi_o}{J} & 0 & 0 \\ -\frac{K_o}{\frac{2}{3}C} & 0 & 0 \end{bmatrix} \tag{6.54}$$

and

$$B = \begin{bmatrix} \frac{U_{do}}{L_L} \\ 0 \\ 0 \end{bmatrix} \tag{6.55}$$

if the non-linear terms are neglected.

It is seen in (6.44) and (6.45) that

$$\frac{dU_d}{dt} = -\frac{3}{2C}\left(\frac{\Psi_o}{J}\delta i_s + \frac{K_o}{J}\delta\omega\right) \tag{6.56}$$

and it can be supposed that

$$\delta U_d = -\frac{3}{2C}\left(\frac{\Psi_o}{J}\delta i_s + \frac{K_o}{J}\delta\omega\right) \tag{6.57}$$

The system can now be reduced to a second order system with $x = (\delta i_s \ \delta\omega)^{\mathrm{T}}$

$$\dot{x} = Ax + Bu =$$

$$= \begin{bmatrix} -\frac{R}{L_L} & -\frac{\Psi_o}{L_L} - \frac{3}{2L_L}\left(\frac{\Psi_o}{J}\right)\left(\frac{K_o}{C}\right)\Psi_o \\ \frac{\Psi_o}{J} & 0 \end{bmatrix} x + \begin{bmatrix} \frac{U_{do}}{L_L} \\ 0 \end{bmatrix} u \tag{6.58}$$

The characteristic polynomial of matrix $A$ is

$$s^2 + \frac{R}{L_L}s + \frac{\Psi_o^2}{JL_L} + \frac{K_o^2}{\frac{2}{3}CJL_L} \tag{6.59}$$

Compare this to equation (6.20). In equation (6.59) a term including the DC link capacitor is added.

The natural frequency and damping are

$$\Omega = \sqrt{\frac{\Psi_o^2}{J \cdot \left( L_L + 2/3 \cdot C \cdot L_L \right)}} \tag{6.60}$$

$$\zeta = \frac{R}{2 \cdot \sqrt{\frac{L_L \cdot \Psi_o}{J \cdot \left( L_L + 2/3 \cdot C \right)}}} \tag{6.61}$$

If the DC link capacitor $C \rightarrow \infty$, the expressions for damping and natural frequency become identical to (6.22) and (6.23).

The smallest value of $C$ and $J$ determines basically the resonance frequency and damping. The damping can not be increased by increasing $C$ if $J$ is small compared to $C$.

One way to increase the damping seems to be to increase the stator resistance, but this is an unfavourable alternative due to two reasons: the losses are increased with additional resistances, and worse, other resonance phenomena might appear. These phenomena are described in the following sections.

To solve the resonance problems some kind of feedback must be used, which is described in a later section.

# 7 Parallel Resonance

A clear mechanical model can be obtained also for the parallel resonance. Computer simulations of the measuring setup show that the amplitudes of the stator, rotor and leakage fluxes are nearly constant at the parallel resonance frequency. To derive a useful model which describes the oscillations, starting with the mechanical model of Fig. 3.5, a few simplifying assumptions are made, based on the results from simulations:

- The rotor resistance is zero in the tangential direction of the rotor. This means that if the rotor flux is turned an angle $\varphi$, the rotor will rotate the same angle $\varphi$ (the slip is zero). However, the rotor drag-pad can move in the radial direction, allowing the motor to be magnetized.
- The leakage inductance $L_L$ is zero.
- The amplitudes of the fluxes are constant
- $u_{sy}$ is constant.

It follows from the assumption $L_L = 0$ that

$$\overline{\Psi}_s = \overline{\Psi}_r = \overline{\Psi} \tag{7.1}$$

This can be described by a mechanical equivalent where the stator and rotor drag-pads are stuck together as if they were one, and this single drag-pad moves in a radial slot i.e. $R_R = 0$ in the tangential direction (Fig. 7.1).

The amplitudes of the fluxes are constant,

$$\Psi = \Psi_s = \Psi_r = \frac{-u_{sy}}{R_s} L_M \tag{7.2}$$

First we make an analysis of this model to determine the natural frequency. Let $\varphi$ denote the angle between the flux and imaginary axis (Fig. 7.2). As the rotor resistance is assumed to be zero, $\varphi$ is also equal to the displacement of the rotor. In this first analysis it is assumed that

$$\Psi \approx - i_{sy} L_M \tag{7.3}$$

The torque is approximately

$$T \approx i_{sy}\ \Psi \sin\varphi \approx -\frac{\Psi^2}{L_M}\sin\varphi \approx -\frac{\Psi^2}{L_M}\varphi \tag{7.4}$$

$$\frac{d\omega}{dt} = \ddot{\varphi} = \frac{T}{J} = -\frac{\Psi^2}{JL_M}\varphi \tag{7.5}$$

The natural frequency is

$$\Omega = \frac{\Psi}{\sqrt{JL_M}} \tag{7.6}$$

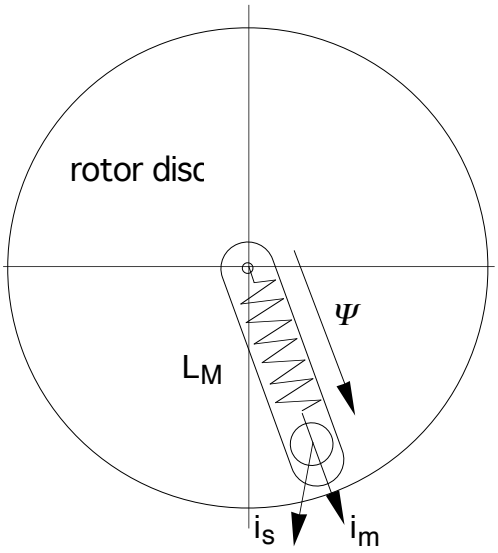


Figure 7.1. Mechanical representation of the parallel resonance

The behaviour of this oscillation can be compared to the behaviour of a pendulum according to Fig. 7.2.

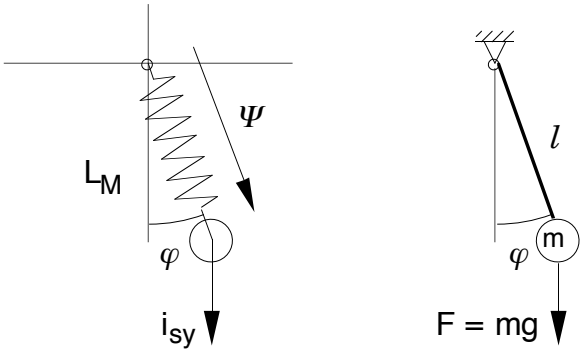


(a) (b)

Figure 7.2 (a) Mechanical representation of parallel resonance (b) Oscillating pendulum

Compare the frequency in equation (7.6) to that of equation (6.22). The only difference between the frequencies is that the leakage inductance in (6.22) is replaced by the magnetizing inductance in (7.6). Physically, the difference is much more significant. The magnetizing inductance $L_M$ influences the resonance frequency, but it is not oscillating in the radial direction, which means that the energy stored in $L_M$ is not oscillating. In the case of the series resonance, the leakage inductance does not only effect the resonance frequency but is also part of the oscillating system, exchanging energy with the rotor of the machine.

This is a system without damping. To find the damping characteristics, the model must be more extensive. The stator equation has to be included. The stator equation is the same as for the complete model of the machine,

$$\frac{d\bar{\Psi}}{dt} = \frac{d\bar{\Psi}_s}{dt} = \bar{u}_s - \bar{i}_s R_s \tag{7.7}$$

As the amplitude of $\bar{\Psi}$ is constant, the flux can only change in a direction perpendicular to itself,

$$\frac{d\bar{\Psi}}{dt} = j\omega\bar{\Psi} \tag{7.8}$$

(7.7) and (7.8) imply

$$\bar{u}_s - \bar{i}_s R_s = j\omega\bar{\Psi} = \omega(-\Psi_{sy} + j\Psi_{sx}) \tag{7.9}$$

If (7.9) is split into real and imaginary parts, (7.10) and (7.11) are obtained,

$$u_{sx} = R_s\, i_{sx} - \omega\, \Psi_{sy} \tag{7.10}$$

$$u_{sy} = R_s\, i_{sy} + \omega\Psi_{sx} \tag{7.11}$$

Equations (7.2), (7.10) and (7.11) give

$$i_{sx} = \frac{\omega}{R_s}\, \Psi_{sy} + \frac{u_{sx}}{R_s} \tag{7.12}$$

$$i_{sy} = -\frac{\omega}{R_s}\, \Psi_{sx} - \frac{\Psi}{L_M} \tag{7.13}$$

The real and imaginary parts of $\bar{\Psi}$ become, according to Fig. 7.2,

$$\Psi_{sx} = \Psi \sin\varphi \tag{7.14}$$

$$\Psi_{sy} = -\Psi \cos\varphi \tag{7.15}$$

The torque can now be expressed as

$$T = Im\,(\bar{\Psi}_s^* \bar{i}_s) = \Psi_{sx}\, i_{sy} - \Psi_{sy}\, i_{sx} =$$

$$= \Psi \cos\varphi \frac{u_{sx}}{R_s} - \Psi^2 \cos^2\varphi \frac{\omega}{R_s} - \Psi^2 \sin^2\varphi \frac{\omega}{R_s} - \frac{\Psi^2}{L_M} \sin\varphi \tag{7.16}$$

If $\varphi$ is small, then $\cos\varphi \approx 1$, $\cos^2\varphi + \sin^2\varphi = 1$ and $\sin\varphi \approx \varphi$, and the torque is

$$T = \Psi \frac{u_{sx}}{R_s} - \Psi^2 \frac{\omega}{R_s} - \frac{\Psi^2}{L_M} \varphi \tag{7.17}$$

The dynamic equations for the system in Fig. 7.1 are

$$\frac{d\omega}{dt} = \frac{T}{J} = \frac{1}{J}\left(\Psi \frac{u_{sx}}{R_s} - \Psi^2 \frac{\omega}{R_s} - \frac{\Psi^2}{L_M} \varphi\right) \tag{7.18}$$

$$\frac{d\varphi}{dt} = \omega \tag{7.19}$$

and can also be written as a second-order differential equation,

$$\ddot{\varphi} + \frac{\Psi^2}{R_s J} \dot{\varphi} + \frac{\Psi^2}{J L_M} \varphi = \Psi \frac{u_{sx}}{J R_s} \tag{7.20}$$

We have the same natural frequency as in (7.6)

$$\Omega = \frac{\Psi}{\sqrt{J L_M}} \tag{7.21}$$

and the relative damping

$$\zeta = \frac{\Psi}{2R_s} \sqrt{\frac{L_M}{J}} \tag{7.22}$$

The parameters of the Grundfos motor (App. B) are inserted into equation (7.21) and (7.22), which give the natural frequency

$$\Omega = \frac{\Psi}{\sqrt{J \cdot L_M}} = \frac{1}{\sqrt{13.5 \cdot 1.6}} = 0.215 \text{ p.u.} = 10.8 \text{ Hz}$$

and the relative damping

$$\zeta = \frac{\Psi}{2R_s}\sqrt{\frac{L_M}{J}} = \frac{1}{2 \cdot 0.07}\sqrt{\frac{1.6}{13.5}} = 2.5$$

Note that a value of damping greater than 1 means that there are no complex poles.

As with the series resonance model, a transfer function from voltage to current can be used to compare the model with measured data. If $\cos\varphi \approx 1$, then (7.12) and (7.15) give

$$i_{sx} = \frac{u_{sx}}{R_s} - \frac{\omega\Psi}{R_s} \tag{7.23}$$

The Laplace transforms of (7.19), (7.20) and (7.23) are

$$s\Phi = W \tag{7.24}$$

$$s^2\,\Phi + \frac{\Psi^2}{R_s \cdot J}s\Phi + \frac{\Psi^2}{J \cdot L_M}\Phi = \Psi\frac{U_{sx}}{J \cdot R_s} \tag{7.25}$$

$$I_{sx} = \frac{U_{sx}}{R_s} - \frac{W\Psi}{R_s} \tag{7.26}$$

and they give

$$I_{sx} = H_p(s)\,U_{sx} = \frac{1}{R_s}\,\frac{s^2 + \frac{\Psi^2}{J \cdot L_M}}{s^2 + \frac{\Psi^2}{R_s \cdot J}s + \frac{\Psi^2}{J \cdot L_M}}\,U_{sx} \tag{7.27}$$

The amplitude and argument of the transfer function $H_p$ for the parallel resonance model is found in Fig. 7.3 (solid). The accordance to the measured data (dashed) is good for frequencies up to the resonance frequency, 0.22 p.u. (10.8 Hz).

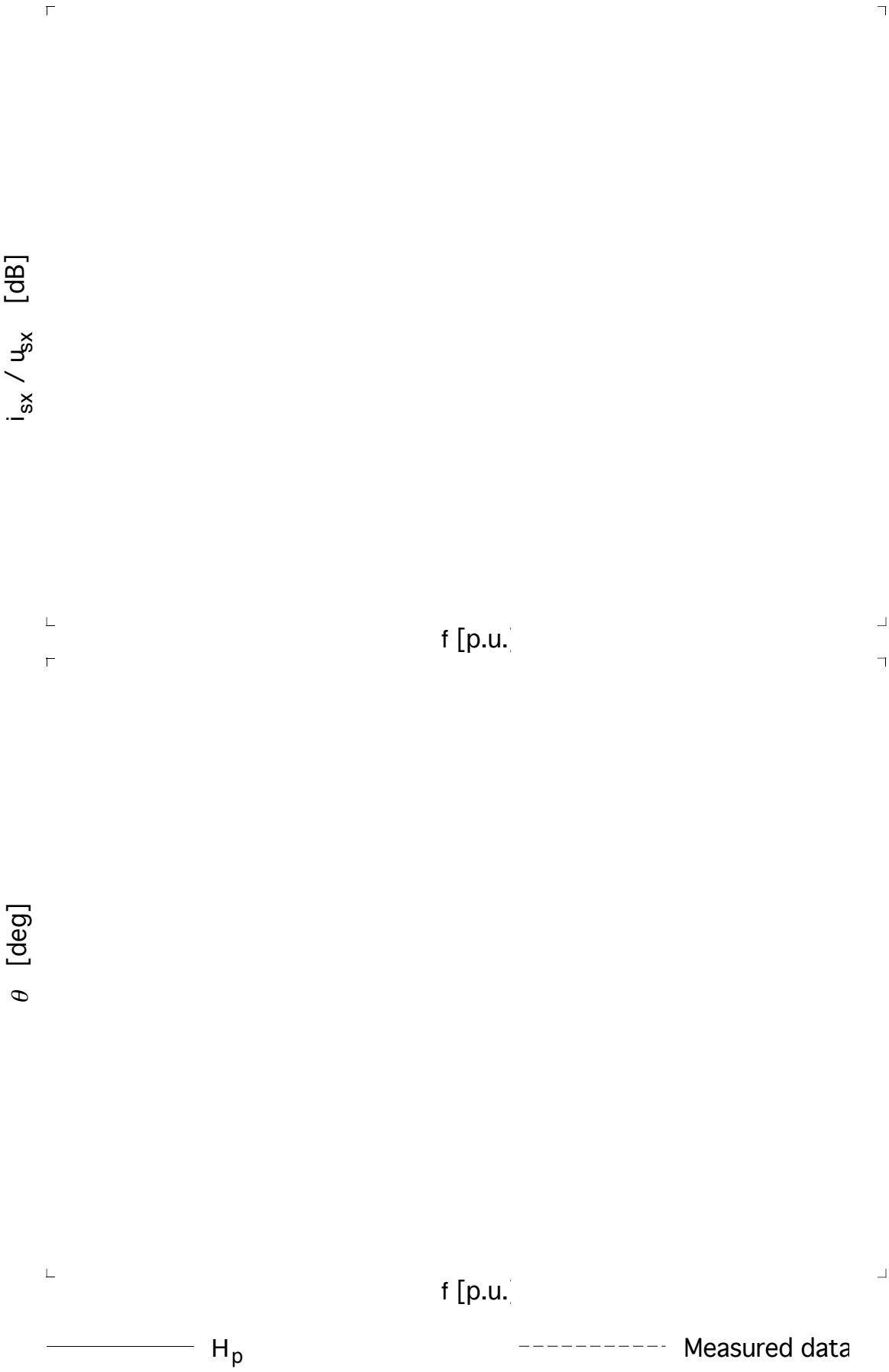


Figure 7.3 Amplitude and argument of transfer function $H_p$

It must be pointed out that since some simplifications are made, the expressions for the resonance frequency do not give exact values, but they describe how the different parameters influence the resonance properties.

The two mechanical models for series resonance (Fig. 6.2) and parallel resonance (Fig. 7.1) can be used to understand the behaviour of the oscillations of the induction machine.

It is important to notice that an increasing stator resistance reduces the damping of the parallel resonance but increases the damping of the series resonance. If MOSFETs are used in the inverter, with a relatively high on-state resistance, this resistance will act as an increased stator resistance, reducing the damping of the parallel resonance.

Another case with high stator resistance is if the motor is fed from long wires. The resistances of the wires in series with the stator windings have the same effect as stator windings with higher resistance.

Trying to solve the series resonance problem by increasing the stator resistance will not only increase the losses but also make the parallel resonance problem worse.

# 8 Linearization

Resonance frequencies of linear systems can be found by computing the eigenvalues of the system matrix. The induction machine is non-linear, and this method can not be used directly. However, the equations describing the machine can be linearized, and the eigenvalues of the linear system can be computed.

This method is in many ways inferior to the methods described earlier in this thesis, as it only results in numerical values but gives no physical insight into the problem. As a comparison, the results of linearization are presented.

To facilitate the linearization, the following time constants are defined:

$$\tau_{ls} = L_L/R_s \tag{8.1}$$

$$\tau_{lr} = L_L/R_R \tag{8.2}$$

$$\tau_{ms} = \frac{\left(\frac{L_M \cdot L_L}{L_M + L_L}\right)}{R_s} = \frac{L_L}{R_s \cdot (1 / (L_M + L_L))} \tag{8.3}$$

$$\tau_{mech} = J\, L_L \tag{8.4}$$

The dynamic equations are rewritten so that the deviation from an operating point, $\Psi_{so}$, $\Psi_{Ro}$, $\omega_o$, is investigated,

$$\bar{\Psi}_s = \bar{\Psi}_{so} + \Delta\bar{\Psi}_s \tag{8.5}$$

$$\bar{\Psi}_R = \bar{\Psi}_{Ro} + \Delta\bar{\Psi}_R \tag{8.6}$$

$$\omega = \omega_o + \Delta\omega \tag{8.7}$$

$$\bar{u}_s = \bar{u}_o + \Delta\,\bar{u} \tag{8.8}$$

At steady state, the stator and rotor fluxes are equal,

$$\bar{\Psi}_{so} = \bar{\Psi}_{Ro} = \bar{\Psi}_o \tag{8.9}$$

The voltage needed at steady state for the flux $\Psi_o$ is

$$\bar{u}_o = \frac{R_s}{L_M}\,\bar{\Psi}_o \tag{8.10}$$

With the equations (8.1-10) inserted into the equations (3.21-3.25), the following equations for the fluxes are obtained,

$$\frac{d\Delta\bar{\Psi}_s}{dt} = \Delta\bar{u} - \frac{1}{\tau_{ms}}\,\Delta\bar{\Psi}_s + \frac{1}{\tau_{ls}}\,\Delta\bar{\Psi}_R \tag{8.11}$$

$$\frac{d\Delta\bar{\Psi}_R}{dt} = \frac{1}{\tau_{lr}}\,\Delta\bar{\Psi}_s - \frac{1}{\tau_{lr}}\,\Delta\bar{\Psi}_R + j\Delta\omega\,\Delta\bar{\Psi}_R + j\Delta\omega\bar{\Psi}_o \tag{8.12}$$

The value of $\Psi_o$ and $\omega_o$ in the tests of section 5 is

$$\Psi_{ox} = 0 \text{ and } \Psi_{oy} = -1 \tag{8.13}$$

$$\omega_o = 0 \tag{8.14}$$

The flux equations, split into real (x) and imaginary (y) parts become

$$\frac{d\Delta\Psi_{sx}}{dt} = \Delta u_x - \frac{1}{\tau_{ms}}\,\Delta\Psi_{sx} + \frac{1}{\tau_{ls}}\,\Delta\Psi_{Rx} \tag{8.15}$$

$$\frac{d\Delta\Psi_{sy}}{dt} = \Delta u_y - \frac{1}{\tau_{ms}}\,\Delta\Psi_{sy} + \frac{1}{\tau_{ls}}\,\Delta\Psi_{Ry} \tag{8.16}$$

$$\frac{d\Delta\Psi_{Rx}}{dt} = \frac{1}{\tau_{lr}}\,\Delta\Psi_{sx} - \frac{1}{\tau_{lr}}\,\Delta\Psi_{Rx} - \underline{\Delta\omega\,\Delta\Psi_{Ry}} + \Delta\omega \tag{8.17}$$

$$\frac{d\Delta\Psi_{Ry}}{dt} = \frac{1}{\tau_{lr}}\,\Delta\Psi_{sy} - \frac{1}{\tau_{lr}}\,\Delta\Psi_{Ry} + \underline{\Delta\omega\,\Delta\Psi_{Rx}} \tag{8.18}$$

and the mechanical equation (3.23) can be written

$$\frac{d\Delta\omega}{dt} =$$

$$\frac{\Delta\Psi_{sx}\left(\underline{\Delta\Psi_{sx}}\,\Delta\Psi_{ry}\right) \quad \Delta\Psi_{rx}\left(\underline{\Delta\Psi_{rx}}\,\Delta\Psi_{sy}\right) \quad T_m}{J \quad L} \tag{8.19}$$

If the non-linear terms, underlined above, are neglected, equations (8.15-8.19) can be replaced by the matrix equation

$$\dot{x} = Ax + Bu$$

or

$$\dot{x} = \begin{bmatrix} -\frac{1}{\tau_{ms}} & 0 & \frac{1}{\tau_{ls}} & 0 & 0 \\ 0 & -\frac{1}{\tau_{ms}} & 0 & \frac{1}{\tau_{ls}} & 0 \\ \frac{1}{\tau_{lr}} & 0 & -\frac{1}{\tau_{lr}} & 0 & 1 \\ 0 & \frac{1}{\tau_{lr}} & 0 & -\frac{1}{\tau_{lr}} & 0 \\ \frac{1}{\tau_{mech}} & 0 & -\frac{1}{\tau_{mech}} & 0 & 0 \end{bmatrix} x + \begin{bmatrix} 1 & 0 & 0 \\ 0 & 1 & 0 \\ 0 & 0 & 0 \\ 0 & 0 & 0 \\ 0 & 0 & \frac{-1}{\tau_{mech}} \end{bmatrix} u \tag{8.20}$$

where

$$x = \begin{bmatrix} \Delta\Psi_{sx} \\ \Delta\Psi_{sy} \\ \Delta\Psi_{Rx} \\ \Delta\Psi_{Ry} \\ \Delta\omega \end{bmatrix} \tag{8.21}$$

and

$$u = \begin{bmatrix} u_{sx} \\ u_{sy} \\ T_m \end{bmatrix} \tag{8.22}$$

The Grundfos motor described in App. B has the following time constants:

$$\tau_{ls} = L_L/R_s = 0.138/0.07 = 1.97$$

$$\tau_{lr} = L_L/R_R = 0.138/0.076 = 1.82$$

$$\tau_{ms} = \frac{1}{R_s(1/L_M + 1/L_L)} = \frac{1}{0.07(1/1.66 + 1/0.138)} = 1.82$$

$$\tau_{mech} = J\,L_L = 13.5 \cdot 0.138 = 1.86$$

which give the matrix $A$ of equation (8.20),

$$A = \begin{bmatrix} -0.55 & 0 & 0.51 & 0 & 0 \\ 0 & -0.55 & 0 & 0.51 & 0 \\ 0.55 & 0 & -0.55 & 0 & 1 \\ 0 & 0.55 & 0 & -0.55 & 0 \\ 0.54 & 0 & -0.54 & 0 & 0 \end{bmatrix}$$

The eigenvalues of this matrix are shown in Fig. 8.1 (a). In (b) are shown the poles of the transfer function $H_s$ from equation (6.26) and in (c) the poles of $H_p$ from equation (7.27),

$$H_s = \frac{s/L_L}{s^2 + \left(\frac{R_r}{L_L} + \frac{\psi^2}{J L_L}\right)s + \frac{R_r}{J L_L}} = \frac{7.25 s}{s^2 + 1.06 s + 0.54}$$

$$H_p = \frac{1}{R_s} \frac{s^2 + \frac{\psi^2}{J L_M}}{s^2 + \left(\frac{\psi^2}{R_s J} + \frac{\psi^2}{J L_M}\right)s + \frac{\psi^2}{J L_M}} = \frac{14.3 s^2 + 0.64}{s^2 + 1.06 s + 0.045}$$

It is seen in the figure that the two poles of $H_s$ lie very close to two of the eigenvalues of $A$, and the two poles of $H_p$ lie close to two other eigenvalues of $A$. This justifies that $H_s$ and $H_p$ give a good description of the oscillatory behaviour of the induction machine.

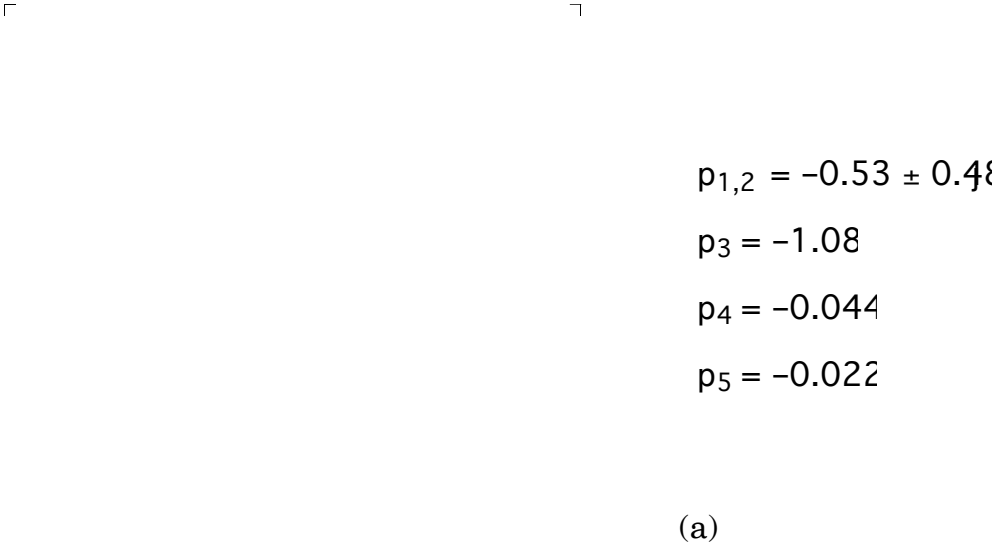


(a)

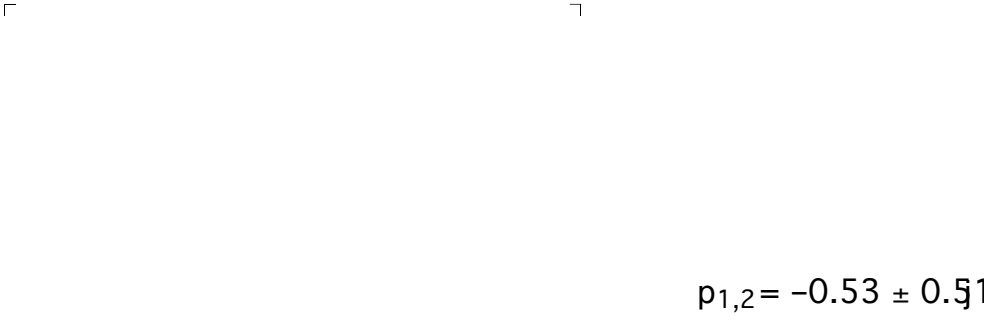


(b)

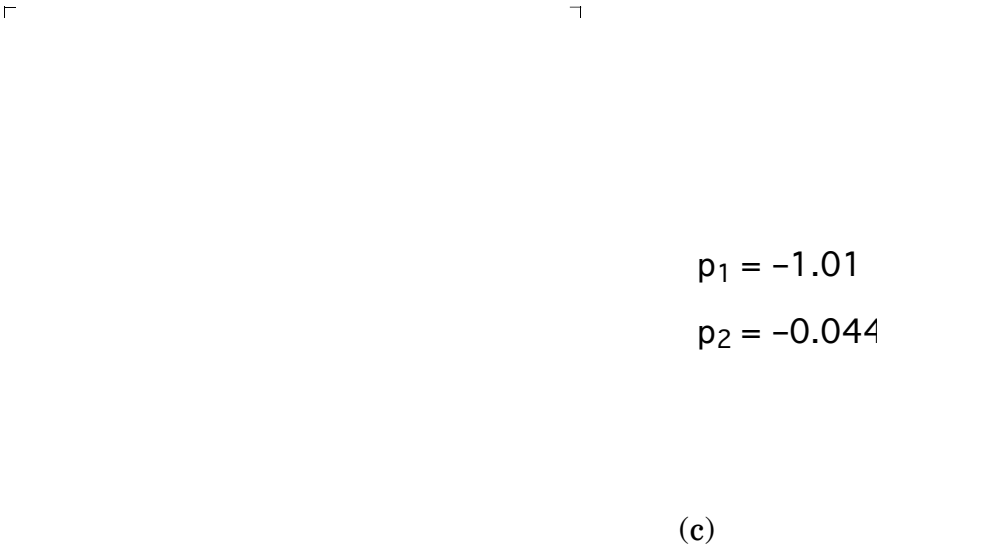


(c)

Figure 8.1 (a) Eigenvalues of matrix $A$ (b) Poles of $H_s$ (c) Poles of $H_p$

# 9 Feedback

Damping of the series resonance described in section 6 can be obtained by feedback. One way is to measure the DC link current $I_d$ and let it control the voltage and stator frequency.

The feasibility of feedback as a way of damping the oscillations is illustrated by a standard proportional controller with gain $G$. The damping of the system described by equation (6.58) can now be chosen arbitrarily. With the feedback law

$$\delta K = -G \cdot \delta i_s \tag{9.1}$$

the damping of the closed-loop system becomes

$$\zeta = \frac{R + G \cdot U_{do}}{2 \cdot \sqrt{\frac{L_L \cdot \Psi_o}{J} \cdot \left(1 + \frac{L_L^2 \cdot K_o}{2/3 \cdot C}\right)}} \tag{9.2}$$

The gain can now be calculated,

$$G = \frac{2 \cdot \zeta \cdot \sqrt{\frac{L_L \cdot \Psi_o}{J} \cdot \left(1 + \frac{L_L^2 \cdot K_o}{2/3 \cdot C}\right)} - R}{U_{do}} \tag{9.3}$$

If for example the damping $\zeta = 1$ is desired for the Grundfos motor at nominal flux with $K_o = 0.58$ and $U_{do} = 1.73$, the gain will be

$$G = 0.0325$$

It is important that the stator frequency $\omega_s$ is adjusted in accordance with the voltage amplitude factor $K$, to get the voltage to frequency ratio constant,

$$\omega_s = \omega_{so} \frac{K}{K_o} \tag{9.4}$$

A simulation of this (App. G) is shown in Fig. 9.1, where (a) shows a start of the motor without feedback, and (b) shows a start with $G = 0.0325$. Note that the oscillation is damped, but that the start is slower with feedback.

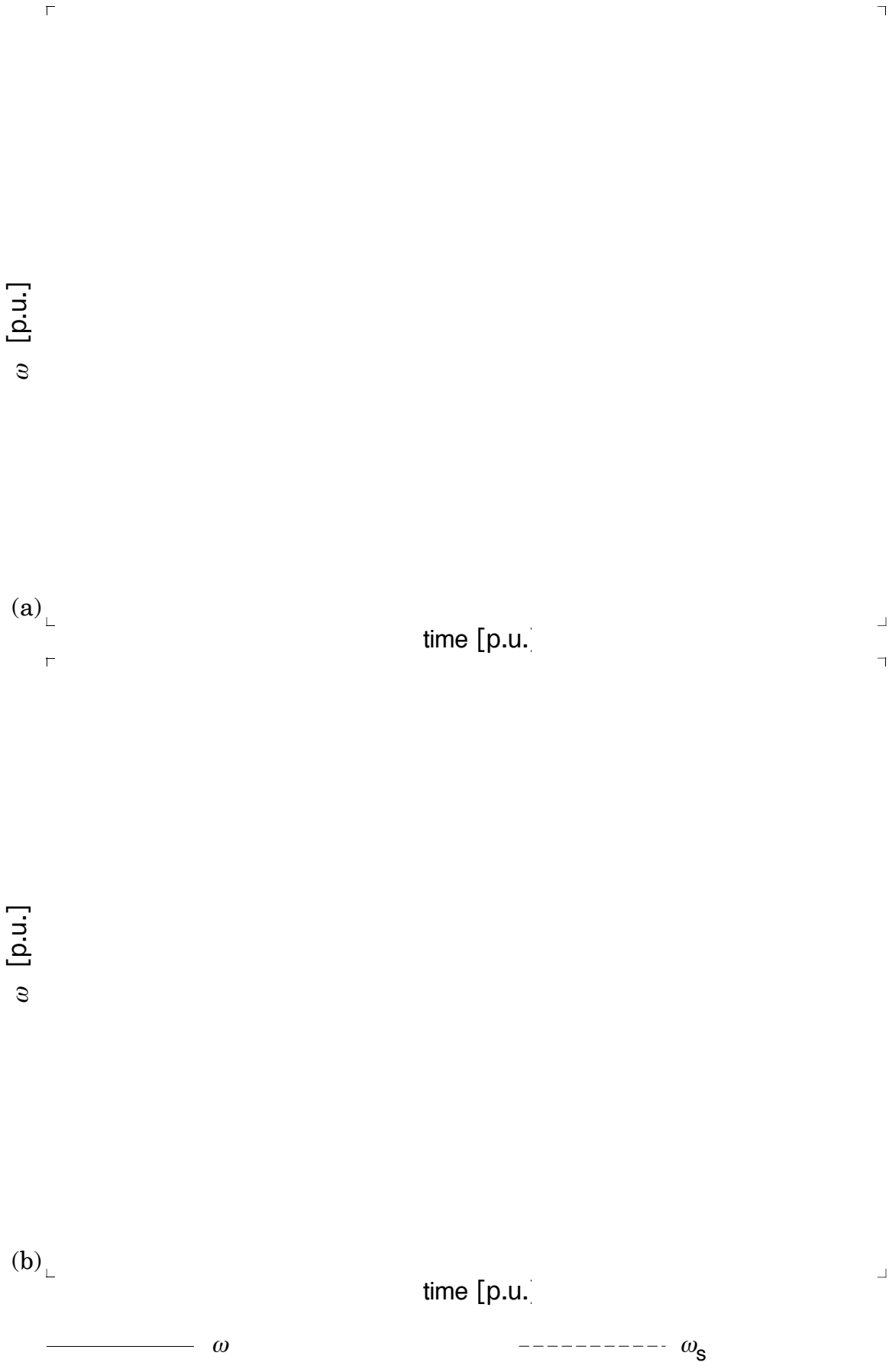


Figure 9.1 Start of induction machine (a) without and (b) with feedback

# 10 Conclusions

The induction machine itself is an oscillating system with different oscillating modes. If the induction machine is connected to an inverter, a torque ripple is introduced that can excite the oscillations. The DC link capacitor of the inverter will also become a part of the oscillating system.

In this thesis, mechanical models are presented which give an intuitive understanding of the different oscillating modes. This understanding is necessary for the design of regulators that can suppress the oscillations. One such regulator is presented which measures only current from the DC link.

# 11 References


1) Alexandrovitz, A. (1987), Determination of Instability Range of a Frequency Controlled Three-Phase Induction Motor Fed Through Series Capacitors, *ETZ Arch*. (Germany), vol. 9, no. 7, July 1987, 235-9.

2) Fitzgerald, A. E., Charles Kingsley, Jr., Stephen D. Umans (1985). *Electric Machinery*, McGraw-Hill, New York.

3) Kovács, P. K. (1984) *Transient phenomena in electrical machines*, Elsevier, Amsterdam.

4) Leonhard, W. (1985). *Control of electrical drives*, Springer, Berlin.

5) Mutoh, N., A. Ueda, K. Sakai, M. Hattori and K. Nandoh (1990). Stabilizing Control Method for Suppressing Oscillations of Induction Motors Driven by PWM Inverters, *IEEE Transactions on Industrial Electronics*, vol. 37, no 1, 48-56

6) Palit, B. B. (1978), Eigenvalue Investigations of a 3-phase Asynchronous Machine with Self-Excited Hunting, *Bull. Assoc. Suisse Electr*. (in German), vol .69, no. 8, 29 April 1978, 371-6.

7) Slemon, G. and A. Straughen (1980). *Electric Machines*, Addison-Wesley, Reading, Mass..

8) Török, V., and J. Valis (1985). *Elektroniska drivsystem* (in Swedish), Tutext, Stockholm.

9) Wagner, C. F. (1930). Effects of Armature Resistance Upon Hunting of Synchronous Machines, *Transactions AIEE*, July 1930.

# Appendix

## A Per Unit Notation

The basic quantities are:

- rated phase voltage $U_n$ (peak value)
- rated phase current $I_n$ (peak value)
- rated electrical angular velocity $\omega_1$
- rated mechanical angular velocity $\omega_n = \omega_1/z_p$
  where $z_p$ is the number of pole pairs
- rated phase flux $\Psi_n = U_n/\omega_1$
- rated apparent power $P_n = 3/2\ U_n\ I_n$
- rated torque $T_n = P_n/\omega_n$
- base impedance $Z_n = U_n/I_n$
- rated start time $H = J\ \omega_n^2/P_n$

The p.u. values of parameters and variables can now be calculated (voltage in p.u. is equal to the voltage in natural units divided by the rated voltage $U_n$ etc):

| | |
|---|---|
| voltage | $u/U_n$ |
| current | $i/I_n$ |
| resistance | $R/Z_n$ |
| inductance | $\omega_1\ L/Z_n$ |
| capacitance | $\omega_1\ C\ Z_n$ |
| flux | $\Psi/\Psi n$ |
| moment of inertia | $\omega_1\ H$ |
| torque | $T/T_n$ |
| time | $\omega_1\ t$ |
| electrical angular velocity | $\omega_{el}\ /\omega_1$ |
| mechanical angular velocity | $\omega_{mech}\ /\omega_n$ |

## B Motor Data

The measurements described in section 4 and 5 have been performed on a Y-connected Grundfos MG 80 B with the following characteristics:

| | |
|---|---|
| rated phase voltage, $U_n$ (peak value) | 310 V |
| rated phase current, $I_n$ (peak value) | 3.82 A |
| rated electrical angular velocity, $\omega_1$ | 314 rad/s |
| number of pole pairs, $z_p$ | 1 |
| rated power, $P$ | 1.1 kW |
| rated power factor, cos $\varphi$ | 0.84 |
| base impedance, $Z_n$ | 81.2 Ω |
| | |
| stator resistance, $R_s$ | 6 Ω |
| rotor resistance, $R_r$ | 6 Ω |
| stator leakage inductance, $L_{sl}$ | 0.0173 H |
| rotor leakage inductance, $L_{rl}$ | 0.0173 H |
| main inductance, $L_m$ | 0.414 H |
| moment of inertia, $J$ | 0.00077 kg m$^2$ |

in p.u. notation:

| | |
|---|---|
| $R_s$ | 0.07 |
| $R_r$ | 0.07 |
| $L_{sl}$ | 0.065 |
| $L_{rl}$ | 0.065 |
| $L_m$ | 1.6 |
| $J$ | 13.5 |
| | |
| $k$ | 0.96 |
| $L_M$ | 1.66 |
| $L_L$ | 0.138 |
| $R_R$ | 0.076 |

## C Vector Equations

For simulation and other purposes, the vector equations (3.21-3.25) can be split up. One way is to separate the real and imaginary parts, another is to separate amplitude and argument of the flux vectors (Fig. C.1).

The following system of five differential equations is obtained if (3.21-3.23) are split into real (x) and imaginary (y) parts :

$$\frac{d\Psi_{sx}}{dt} = u_{sx} - i_{sx} R_s$$

$$\frac{d\Psi_{sy}}{dt} = u_{sy} - i_{sy} R_s$$

$$\frac{d\Psi_{Rx}}{dt} = -\omega \Psi_{Ry} - i_{Rx} R_R$$

$$\frac{d\Psi_{Ry}}{dt} = \omega \Psi_{Rx} - i_{Ry} R_R$$

$$\frac{d\omega}{dt} = \frac{\Psi_{sx} \cdot i_{sy} - \Psi_{sy} \cdot i_{sx}}{J}$$

Note that these equations are written in the stator reference frame.

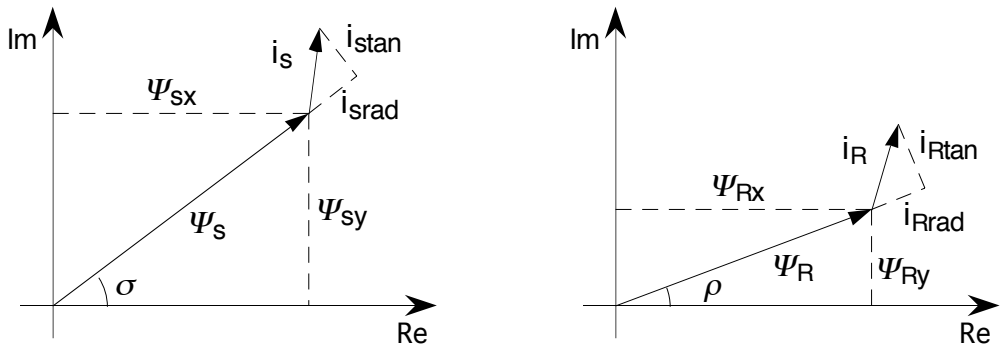


(a) (b)

Figure C.1 Flux and current vectors and their components
(a) Stator (b) Rotor

The stator and rotor flux vectors can be expressed with amplitudes and arguments,

$$\bar{\Psi}_s = \Psi_s \, \mathrm{e}^{j\sigma}$$

$$\bar{\Psi}_R = \Psi_R \, \mathrm{e}^{j\rho}$$

Let the index *rad* represent components pointing in the *radial* direction, parallel to the flux, and the index *tan* represent components in the *tangential* direction, perpendicular to the flux. This means for example that $i_{srad}$ is the x-component of the stator current expressed in a reference frame attached to the stator flux, and $i_{stan}$ is the corresponding y-component. The equations (3.21-3.25) can be written as five differential equations and some algebraic relations,

$$\frac{d\Psi_s}{dt} = u_{srad} - R_s \, i_{srad}$$

$$\frac{d\sigma}{dt} = (u_{stan} - R_s \, i_{stan})/\Psi_s$$

$$\frac{d\Psi_R}{dt} = -\, i_{Rrad} \, R_R$$

$$\frac{d\rho}{dt} = (\Psi_R \, \omega - i_{Rtan})/\Psi_R$$

$$\frac{d\omega}{dt} = \Psi_s \, i_{stan} \, / \, J$$

$$i_{srad} = \Psi_s/L_M - \Psi_s/L_L - \Psi_R \cos\delta/L_L$$

$$i_{stan} = \Psi_R \sin\delta/L_L$$

$$i_{Rrad} = \Psi_R/L_L - \Psi_s \cos\delta/L_L$$

$$i_{Rtan} = -\Psi_s \sin\delta/L_L$$

$$\delta = \sigma - \rho$$

The following two relations transform the stator voltage from coordinates in the stator reference frame to the stator *flux* reference frame,

$$u_{srad} = u_{sx} \cos\sigma + u_{sy} \sin\sigma$$

$$u_{stan} = -u_{sx} \sin\sigma + u_{sy} \cos\sigma$$

## D Coordinate Transformations

The vector equations can be transformed to a coordinate system rotating with the angular velocity $\omega_k$. The quantities in the rotating system are denoted by a superscript-k. The angle between the rotating system, and the coordinate system fixed to the stator is denoted by $\varphi$. It follows that

$$\frac{d\varphi}{dt} = \omega_k$$

$$\bar{\Psi}_s = \bar{\Psi}_s^k \, \mathrm{e}^{j\varphi}, \; \bar{i}_s = \bar{i}_s^k \, \mathrm{e}^{j\varphi} \text{ etc.}$$

$$\frac{d\bar{\Psi}_s}{dt} = \frac{d\bar{\Psi}_s^k}{dt} \, \mathrm{e}^{j\varphi} + j \, \frac{d\varphi}{dt} \, \bar{\Psi}_s^k \, \mathrm{e}^{j\varphi}$$

$$\frac{d\bar{\Psi}_r}{dt} = \frac{d\bar{\Psi}_r^k}{dt} \, \mathrm{e}^{j\varphi} + j \, \frac{d\varphi}{dt} \, \bar{\Psi}_r^k \, \mathrm{e}^{j\varphi}$$

If these relations are inserted into the vector equations in stator coordinates, the following equations are obtained,

$$\frac{d\bar{\Psi}_s^k}{dt} = \bar{u}_s^k - \bar{i}_s^k \, R_s - j \, \omega_k \, \bar{\Psi}_s^k$$

$$\frac{d\bar{\Psi}_r^k}{dt} = j\omega\bar{\Psi}_r^k - \bar{i}_r^k \, R_r - j \, \omega_k \, \bar{\Psi}_r^k$$

The torque equation is invariant against coordinate transformations.

## E Mechanical Analogy

An electric motor is both an electrical and a mechanical system. The interaction between the electrical and mechanical parts are often complicated to analyze. By representing the electrical part of the system by its mechanical analogy, the complete system becomes mechanical and more easy to analyze.

If the product of two quantities in the electrical system yields power, then the product of the corresponding mechanical quantities must be power. In the electrical system, the product of current and voltage is power. If current is represented for example by force the voltage should be represented by speed as the product of force and speed is power. This gives a very useful mechanical analogy. The table below shows some other corresponding electrical and mechanical quantities, as well as mechanical components corresponding to the electrical ones.

| Electrical system | Mechanical equivalent |
|---|---|
| power $P$ [W] | power $P$ [W] |
| current $i$ [A] | force $F$ [N] |
| voltage $u$ [V] | speed $v$ [m/s] |
| linked flux $\Psi$ [Vs] | distance $x$ [m] |
| resistance $R$ [Ω] | inverse of damping $1/d$ [m/Ns] |
| inductance $L$ [H] | inverse of spring stiffness $1/k$ [m/N] |
| capacitance $C$ [F] | mass $m$ [kg] |

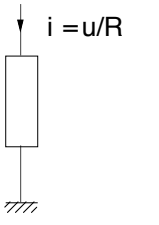


resistance

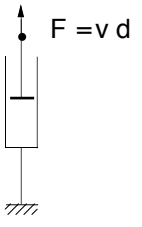


viscous damper

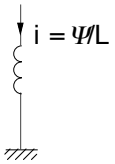


inductance

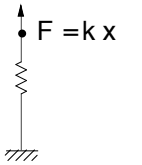


spring

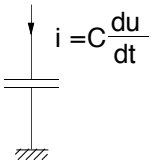


capacitance

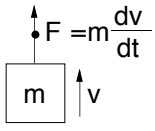


mass

## F Roots, Natural Frequency and Damping

The equation

$$s^2 + 2\Omega\zeta s + \Omega^2 = 0$$

has the roots

$\zeta<1$: $$s = -\Omega\zeta \pm j\sqrt{1-\zeta^2}$$

$\zeta>1$: $$s = -\Omega\zeta \pm \sqrt{\zeta^2-1}$$

In the case of complex roots, they can be demonstrated by Fig. F.1. $\Omega$ is the *natural frequency* and $\zeta$ is the *damping*.

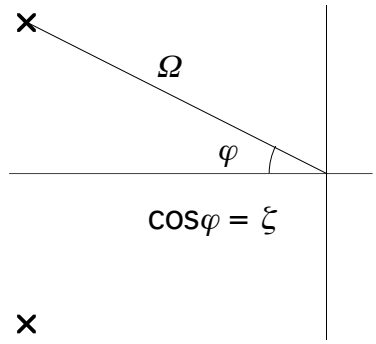


Figure F.1 Relation between location of roots, natural frequency and damping

Figure F.2 shows the time variation of the state variable $x$ of the system

$$\ddot{x} + 2\Omega\zeta\dot{x} + \Omega x = 0$$

with the initial value $x_o = 1$. The natural frequency $\Omega = 1$, the damping $\zeta = 0.1$ for the solid line, and $\zeta = 1$ for the dashed line. The dotted line shows

$$e^{-\zeta\Omega t}; \quad \zeta = 0.1, \Omega = 1$$

The frequency of oscillation for $\zeta = 0.1$ is

$$\omega = \Omega\sqrt{1-\zeta^2} = 0.995 \text{ rad/s}$$

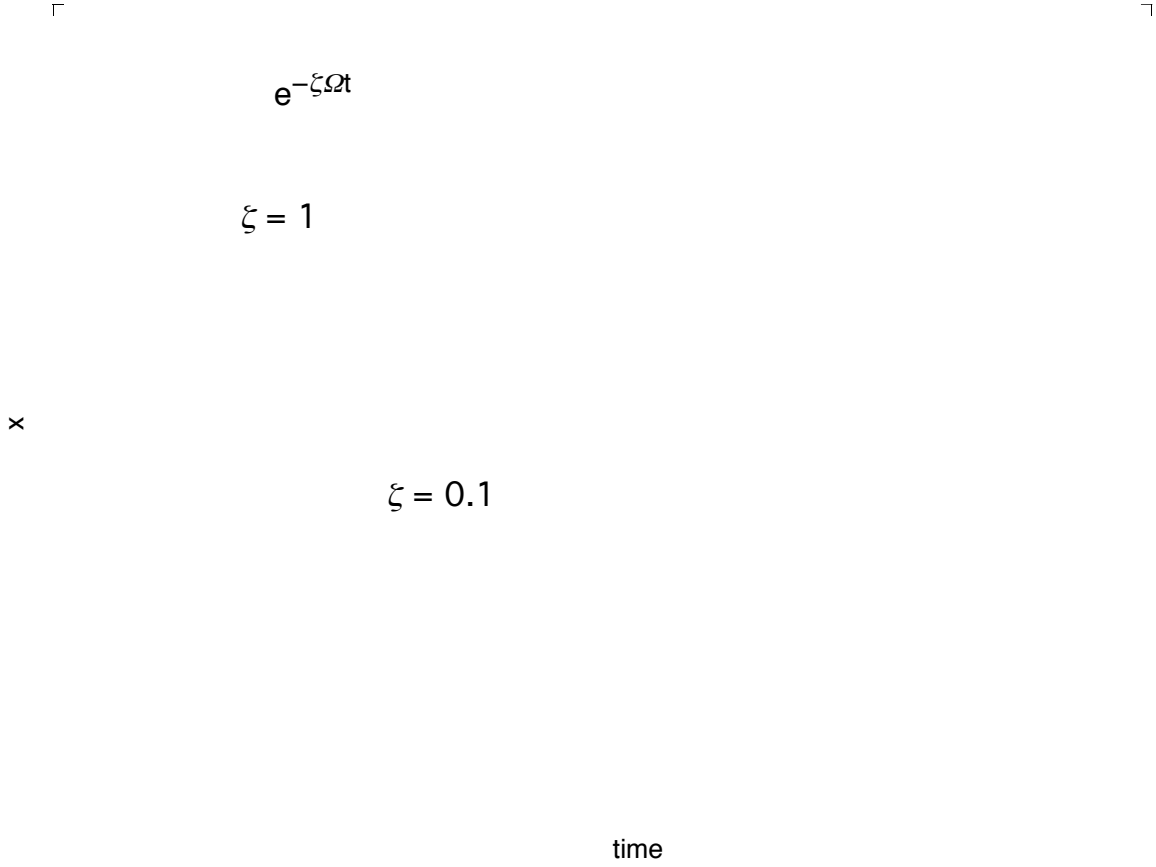


Figure F.2 Simulation of $\ddot{x} + 2\Omega\zeta\dot{x} + \Omega x = 0$

## G Simulation File

The simulations have been performed with the program Simnon™. The following file is used to simulate the start of an induction motor with and without feedback.

```
continuous system feedback
"gamma model of induction machine in p.u. notation
"stator coordinates
"DC link current feedback

"stator flux, rotor flux, angular velocity, rotor angle,
"arg of stator voltage
state psisx  psisy  psirx  psiry  w  theta  argu
der   dpsisx dpsisy dpsirx dpsiry dw dtheta dargu

time t

"Grundfos parameters in p.u.
LM:1.6
LL:0.138
Rs:0.07
Rr:0.076
J:13.5
Tload:0
zero:0
psin:1 "nominal flux

Ud:1.73
K0:0.58
ws0:1 "stator frequency


"feedback
deltaK=-gain*deltaId*2/3/K0
K=K0+deltaK
u=K*Ud
ws=ws0*K/K0
Id0:0.0273
Id=is*cos(argis-argu)
deltaId=Id-Id0
gain:0.0325

"feeding voltage
dargu=ws
usx=u*cos(argu)
usy=u*sin(argu)

us=sqrt(sqr(usx)+sqr(usy))
```

```
"dynamic equations
dpsisx=usx-Rs*isx
dpsisy=usy-Rs*isy
dpsirx=-w*psiry-Rr*irx
dpsiry= w*psirx-Rr*iry
dw=(Torque-Tload)/J
dtheta=w

imx=psisx/Lm
imy=psisy/Lm
im=sqrt(imx*imx+imy*imy)
argim=atan2(imy,imx)
irx=(psirx-psisx)/LL
iry=(psiry-psisy)/LL
argir=atan2(iry,irx)
ir=sqrt(irx*irx+iry*iry)
isx=imx-irx
isy=imy-iry
is=sqrt(isx*isx+isy*isy)
argis=atan2(isy,isx)
Torque=(psisx*isy-psisy*isx)

P2=w*Torque
P1=(3/2)*(usx*isx+usy*isy)

"rotating reference frame
fi0:-0.17
fi=ws*t-fi0
cfi=cos(fi)
sfi=sin(fi)
psisxr= psisx*cfi+psisy*sfi
psisyr=-psisx*sfi+psisy*cfi
psirxr= psirx*cfi+psiry*sfi
psiryr=-psirx*sfi+psiry*cfi

end
```

## H List of Symbols

| | |
|---|---|
| amplitude factor | $K$ |
| angular velocity | $\omega$ |
| capacitance | $C$ |
| current | $i$ |
| rotor current | $i_r$, $i_R$ |
| stator current | $i_s$ |
| line current | $i_a$, $i_b$, $i_c$ |
| frequency | $f$ |
| stator frequency | $f_s$, $\omega_s$ |
| inductance | $L$ |
| mutual inductance | $L_m$, $L_M$ |
| rotor leakage inductance | $L_{rl}$ |
| stator leakage inductance | $L_{sl}$ |
| Laplace operator | $s$ |
| linked flux | $\Psi$ |
| rotor flux | $\Psi_r$, $\Psi_R$ |
| stator flux | $\Psi_s$ |
| moment of inertia | $J$ |
| natural frequency | $\Omega$ |
| power factor | $\cos\varphi$ |
| relative damping | $\zeta$ |
| resistance | $R$ |
| rotor resistance | $R_r$, $R_R$ |
| stator resistance | $R_s$ |
| slip | $s$ |
| pull-out slip | $s_p$ |
| time constant | $\tau$ |
| time | $t$ |
| torque | $T$ |
| load torque | $T_m$ |
| pull-out torque | $T_p$ |
| voltage | $u$ |
| stator voltage | $u_s$ |
| phase-to-neutral voltage | $u_a$, $u_b$, $u_c$ |

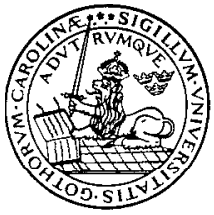


CODEN: LUTEDX/(TEIE-1001)/1-67/(1991)

Efter sista sidan